ability to inhibit replication of HCV RNA via specific antiviral mechanism(s).

Anti-HCV Activity of Statins Not Due to Inhibition of RL Activity. We clearly showed that the anti-HCV activities of statins were not due to their cytotoxicity. However, it remained to be clarified whether the statins used in this study would directly inhibit RL activity, because we recently found that two antifungal compounds, amphotericin B (AMPH-B) and nystatin, drastically inhibited RL activity (Ikeda et al., unpublished data). To examine this possibility, we investigated the effects of statins on RL activity. The addition of the statins to cell lysates prepared from OR6 cells revealed that none of the statins (up to 10 μmol/L) tested exhibited any inhibitory effect on RL activity, although AMPH-B extensively inhibited RL activity (Fig. 3C). This result excludes the possibility that the statins directly inhibit RL activity.

Anti-HCV Activity of Statins Not Due to Inhibition of EMCV IRES Activity. To further exclude the possibility that the anti-HCV activities of statins were a result of the artificial assay system, we next tested the possibility that the statins inhibit EMCV IRES activity, because Core-NS5B is translated in an EMCV-IRES-dependent manner in OR6 cells. The plasmid encoding RL driven by EMCV IRES was transfected into the OR6c cells, and 24 hours after transfection the cells were treated with each statin (5 μmol/L each) for 72 hours. The results revealed none of the statins exhibited any inhibitory effect, although AMPH-B drastically inhibited RL activity again (Fig. 3D). These data suggest the statins had no effect on exogenous genes EMCV IRES and RL introduced into HCV RNA.

Statins Prevent Replication of Authentic HCV RNA. To obtain further evidence that the statins prevent HCV RNA replication, we prepared authentic HCV-O-derived genome-length HCV RNA possessing two adaptive mutations (HCV-O/KE/EG). One adaptive mutation, K1609E in NS3, was previously described,[9] and the other, E1202G in NS3, was found in OA cells harboring genome-length HCV-O RNA (Abe et al., in preparation). The combination of these two mutations markedly enhanced the efficiency of HCV RNA replication, and HCV proteins were continuously detected for at least 8 weeks (Abe et al., in preparation). HCV-O/dGDD, from which the GDD motif in NS5B polymerase was deleted, was used as a control. HCV-O/KE/EG and HCV-O/dGDD RNAs were transfected into OR6c cells, and the production of HCV proteins was monitored for 96 hours. The Core and NS3 in the OR6c cells transfected with HCV-O/dGDD RNA were not detected even 96 hours after transfection. However, the Core and NS3 in the OR6c cells transfected with HCV-O/KE/EG RNA were detected 24 hours after transfection, and their expression increased with time (Fig. 3E). This observation suggests that HCV-O/KE/EG RNA, without exogenous genetic factors such as EMCV IRES and RL, efficiently replicates in OR6c cells. Using such a transient HCV RNA replication system, we demonstrated that the production of Core and NS3 was markedly prevented when the OR6c cells transfected with HCV-O/KE/EG RNA were treated with FLV (5 μmol/L) at 24 hours after transfection (Fig. 3E). In summary, our results indicate that the statins prevent HCV RNA replication and that their inhibitory effects are not a result of the inhibitory effect toward the exogenous genes introduced into ORN/C-5B RNA replicating in OR6 cells.

Combination of a Statin with IFN Efficiently Enhances Anti-HCV Activity of IFN. IFN is the world standard of therapy for CH C, and currently its best partner is ribavirin. Because we found the statins efficiently inhibited HCV activity, we expected the statins to be candidates for use in combination with IFN. To address this point, we examined the inhibitory effects of combinations of IFN-α (0, 2, 4, and 8 IU/mL) and the statins (5 μmol/L each) using the OR6 assay system. As expected, ATV, SMV, FLV, and LOV markedly enhanced the anti-HCV effect of IFN-α, although PRV did not (Fig. 4A). In combination with IFN-α, FLV again was the statin that had the strongest effect. The results indicated that cotreatment was more effective than treatment with IFN-α alone. We thought the mechanism underlying this phenomenon might be statin-induced enhancement of the type I IFN signaling pathway. To examine this possibility, we investigated the phosphorylation status of STAT1 after statin treatment. The results revealed that FLV did not cause phosphorylation of STAT1 in OR6c or OR6 cells, although IFN-α did so efficiently in both types of cells (Fig. 4B). In addition, we confirmed that phosphorylation of STAT2 and STAT3 in both cell types was also not induced by FLV treatment (data not shown). Furthermore, we confirmed that FLV did not affect expression of 2′-5′-OAS1 mRNA and that the expression level induced by IFN-α treatment was not affected by treatment with FLV (Fig. 4C). PRV, which showed no anti-HCV activity, also had no effect on the type I IFN signaling pathway. In summary, these results indicate the statin-induced enhancement of the anti-HCV action of IFN-α is not a result of induction of the type I IFN signaling pathway.

Cotreatment of IFN-α and FLV Exhibits Synergistic Inhibitory Effects on HCV RNA Replication. We showed that FLV was the statin tested that exhibited the strongest anti-HCV activity, not only alone, but also in combination with IFN-α. Therefore, we focused on the anti-HCV activity of FLV, minutely examining the in-

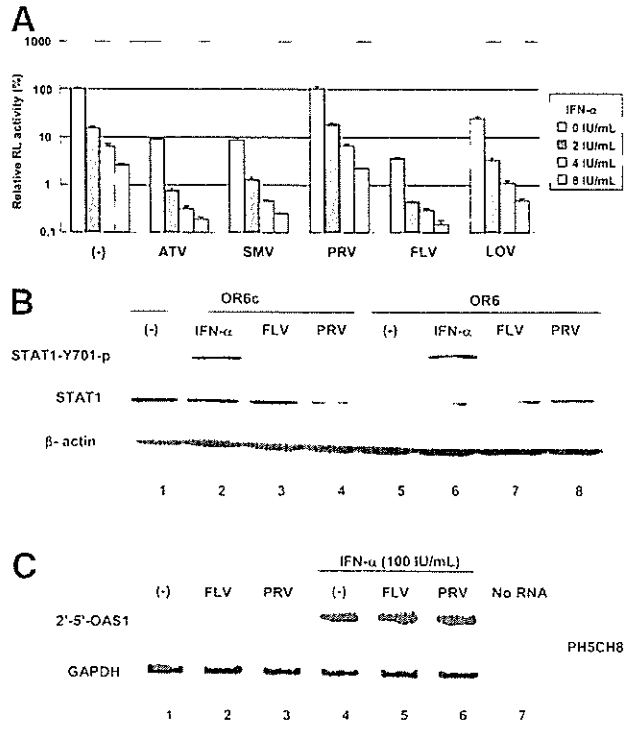

Fig. 4. Statins enhance inhibition of HCV RNA replication because of IFN-α. (A) Effects of statins on the anti-HCV activity of IFN. OR6 cells were cotreated with IFN-α (0, 2, 4, and 8 IU/mL) and ATV, SMV, PRV, FLV, or LOV (5 μmol/L each). The RL assay was performed, and the relative RL activity was calculated as shown in Fig. 1B. (B) No enhancement of type I IFN signaling by the statins. OR6c or OR6 cells were cultured for 2 hours in the absence and in the presence of IFN-α (100 IU/mL), FLV (10 μmol/L), and PRV (10 μmol/L), and the cells were subjected to Western blot analysis of STAT1 and its phosphorylation status. β-actin was used as a control for the amount of protein loaded per lane. (C) No induction of the IFN-inducible gene by the statins. PH5CH8 cells were untreated or were treated with FLV (10 μmol/L) and PRV (10 μmol/L) for 2 hours, and then total RNA extracted from the cells was subjected to RT-PCR for 2′-5′-OAS1 (25 cycles). The PH5CH8 cells were treated for 9 hours with IFN-α (100 IU/mL) alone or in combination with FLV (10 μmol/L) or PRV (10 μmol/L), and then RT-PCR for 2′-5′-OAS1 was performed. The RT-PCR products (358 bp for 2′-5′-OAS1 and 334 bp for GAPDH) were detected, as shown in Fig. 1D.

hibitory effects of the combination of IFN-α and FLV on genome-length HCV RNA replication. A dose-response curve of FLV was obtained for fixed concentrations of IFN-α of 0, 4, 8, 16, 32, and 64 IU/mL. The results revealed the curves shifted to shift markedly to the bottom as the concentration of IFN-α increased (Fig. 5A), indicating that cotreatment was drastically more effective than treatment with IFN-α alone. Furthermore, we observed that RL activity decreased to almost the background level in the OR6 reporter assay when OR6 cells were cotreated with 64 IU/mL of IFN-α and FLV at concentrations above 1.25 μmol/L (Fig. 5A). Because the data in Fig. 5A indicate the possibility of a synergistic effect of the combination of IFN-α and FLV, we examined whether the effect of this combination is synergistic or additive effect using an isobologram method.[23,24] The anti-HCV activities of IFN-α and FLV in combination were evaluated by the OR6 reporter assay. Dose-response inhibition of HCV RNA replication was evaluated for varying IFN-α concentrations (0-8 IU/mL) in the presence of various doses of FLV (0-7.5 μmol/L). The IC_{90} values of IFN-α and FLV were 4.0 IU/mL and 6.7 μmol/L, respectively. These data were used to generate isoboles, which demonstrated 90% inhibition of HCV RNA replication, and the synergistic anti-HCV action of IFN-α and FLV was revealed by the curvilinear plots of the 90% isoboles (Fig. 5B). In conclusion, we clearly demonstrated that combination treatment of IFN-α and FLV was an overwhelmingly more effective treatment,

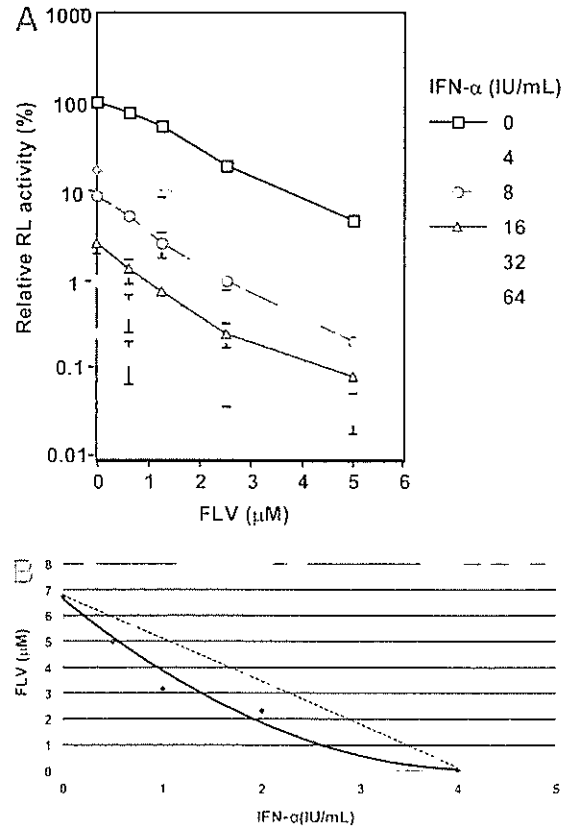

Fig. 5. Synergistic effect of FLV in combination with IFN-α on HCV RNA replication. (A) Effect of FLV in combination with IFN-α. OR6 cells were cotreated with FLV (0, 0.625, 1.25, 2.5, and 5 μmol/L) and IFN-α (0, 4, 8, 16, 32, and 64 IU/mL). The RL assay was performed after 72 hours of treatment, and the relative RL activity was calculated as shown in Fig. 1B. (B) Isobole plots of 90% inhibition of HCV RNA replication. OR6 cells were treated with IFN-α (0, 0.5, 1, 2, 4, 6, and 8 IU/mL) in combination with FLV (0, 0.625, 1.25, 2.5, 5, and 7.5 μmol/L) for 72 hours, and the RL assay was performed as shown in Fig. 1B to obtain 90% isoboles. The broken line indicates the additive effect in the isobologram method used.[23,24]

compared with the previous results for the combination treatment of IFN-α with ribavirin.[10]

Discussion

In this study, we found that different statins have different anti-HCV profiles. FLV, ATV, and SMV each exerted a stronger inhibitory effect on HCV RNA replication than did that of LOV reported previously.[11,12] However, PRV exhibited no anti-HCV activity. We also demonstrated that anti-HCV activity was drastically increased when these statins except PRV were used in combination with IFN-α. Because these statins are currently used for the clinical treatment of patients with hypercholesterolemia without inducing severe side effects, our findings suggest that these statins might be useful in combination therapy with IFN-α or IFN-α plus ribavirin.

That PRV exhibited no anti-HCV activity is interesting. From the information on LOV only[10,11] to date, the mechanism underlying statins' inhibition of HCV RNA replication has not been considered their cholesterol-lowering activity but rather their inhibition of geranylgeranylation of cellular proteins. In other words, statins' inhibition of HMG-CoA reductase leads to the reduction of intracellular mevalonate and consequently to a reduction in geranylgeranyl pyrophosphate. In fact, in OR6 cells we observed that mevalonate and geranylgeraniol restored HCV RNA replication in the FLV- or LOV-treated cells. However, we found unexpectedly that PRV did not inhibit HCV RNA replication, whereas PRV inhibited HMG-CoA reductase as effectively as other statins possessing anti-HCV activity. Although PRV is a water-soluble reagent (others are lipophilic), we confirmed PRV did induce expression of HMG-CoA reductase by a positive feedback mechanism[18] and LST-1 was expressed in our cell culture system. These findings suggest the presence of a mechanism in which PRV's inhibition of HMG-CoA reductase does not cause the depletion of geranylgeranyl pyrophosphate. Interestingly, it has been reported that PRV has a unique effect among statins on the induction of p450.[18] Therefore, further studies are needed to explain why PRV exhibits no anti-HCV activity.

We minutely examined the effect of FLV, the statin exhibiting the strongest inhibition of HCV replication of those tested in this study, in combination with IFN-α. We found that a combination treatment of IFN-α and FLV had a synergistic inhibitory effect on HCV RNA replication. Although high doses of IFN-α are more effective than low doses for eliminating HCV from a patient, the side effects increase in a dose-dependent manner. Because ribavirin enhances the effect of IFN-α slightly in a cotreatment, it is the only reagent currently used with IFN-α to treat patients with CH C. In our previous study of anti-HCV activity using the OR6 assay system, we found the IC_{50} of ribavirin to be 76 μmol/L.[10] This concentration is much higher than the clinically achievable ribavirin concentration (10-14 μmol/L) previously reported.[25] Furthermore, when administered in combination with IFN-α (2 IU/mL) and ribavirin (50 μmol/L), HCV RNA replication was reduced by only approximately 50%, compared with the effect of treatment with IFN-α alone.[10] It has been reported that the maximum blood concentration of FLV after 40 mg/day being administered orally for 4 weeks is approximately 0.6 μmol/L.[26] This concentration is rather low for the inhibition of HCV replication *in vivo*, because the IC_{90} of FLV was assigned as 6.7 μmol/L in our assay system (Fig. 5B). In addition, our study showed reatment of OR6 cells with 5 μmol/L FLV alone was almost equal to the effect of 10 IU/mL IFN-α. Although statins are known to concentrate in the liver, FLV monotherapy will not be effective for patients with CH C. However, we demonstrated that the combination of IFN-α and FLV exhibited synergistic effects on HCV RNA replication. For example, when administered in combination with IFN-α (2-8 IU/mL) and FLV (5 μmol/L), HCV RNA replication fell remarkably, to approximately 3%, compared with the effects of treatment with IFN-α alone (Fig. 4A). From these results, we propose that therapy combining FLV with IFN-α may be effective for the treatment of patients with CH C. Furthermore, additional treatment with reagents in combination (e.g., IFN-α, ribavirin, and FLV) will help to improve the SVR rate.

In conclusion, the results of the present study suggest that statins other than PRV are good reagents for combination therapy with IFN-α in patients with CH C. Although the mechanism by which PRV lacks anti-HCV activity has not been clarified in the present study, a better understanding of this mechanism may lead to the discovery of statin-related anti-HCV reagents possessing no cholesterol-lowering activity. Furthermore, our developed OR6 assay system will be useful for the time-saving screening of new anti-HCV reagents.

Acknowledgment: The authors thank Atsumi Morishita and Takashi Nakamura for their technical assistance.

References

1. Feld JJ, Hoofnagle JH. Mechanism of action of interferon and ribavirin in treatment of hepatitis C. Nature 2005;436:967-972.
2. Lohmann V, Korner F, Koch J, Herian U, Theilmann L, Bartenschlager R. Replication of subgenomic hepatitis C virus RNAs in a hepatoma cell line. Science 1999;285:110-113.
3. Ikeda M, Yi M, Li K, Lemon SM. Selectable subgenomic and genome-length dicistronic RNAs derived from an infectious molecular clone of the

HCV-N strain of hepatitis C virus replicate efficiently in cultured Huh7 cells. J Virol 2002;76:2997-3006.
4. Pietschmann T, Lohmann V, Kaul A, Krieger N, Rinck G, Rutter G, Strand D, et al. Persistent and transient replication of full-length hepatitis C virus genomes in cell culture. J Virol 2002;76:4008-4021.
5. Yi M, Bodola F, Lemon SM. Subgenomic hepatitis C virus replicons inducing expression of a secreted enzymatic reporter protein. Virology 2002;304:197-210.
6. Wakita T, Pietschmann T, Kato T, Date T, Miyamoto M, Zhao Z, et al. Production of infectious hepatitis C virus in tissue culture from a cloned viral genome. Nat Med 2005;11:791-796.
7. Lindenbach BD, Evans MJ, Syder AJ, Wolk B, Tellinghuisen TL, Liu CC, et al. Complete replication of hepatitis C virus in cell culture. Science 2005;309:623-626.
8. Zhong J, Gastaminza P, Cheng G, Kapadia S, Kato T, Burton DR, et al. Robust hepatitis C virus infection in vitro. Proc Natl Acad Sci U S A 2005;102:9294-9299.
9. Ikeda M, Abe K, Dansako H, Nakamura T, Naka K, Kato N. Efficient replication of a full-length hepatitis C virus genome, strain O, in cell culture, and development of a luciferase reporter system. Biochem Biophys Res Commun 2005;329:1350-1359.
10. Naka K, Ikeda M, Abe K, Dansako H, Kato N. Mizoribine inhibits hepatitis C virus RNA replication: effect of combination with interferon-alpha. Biochem Biophys Res Commun 2005;330:871-879.
11. Ye J, Wang C, Sumpter R Jr, Brown MS, Goldstein JL, Gale M Jr. Disruption of hepatitis C virus RNA replication through inhibition of host protein geranylgeranylation. Proc Natl Acad Sci U S A 2003;100:15865-15870.
12. Kapadia SB, Chisari FV. Hepatitis C virus RNA replication is regulated by host geranylgeranylation and fatty acids. Proc Natl Acad Sci U S A 2005; 102:2561-2566.
13. Wang C, Gale M Jr, Keller BC, Huang H, Brown MS, Goldstein JL, et al. Identification of FBL2 as a geranylgeranylated cellular protein required for hepatitis C virus RNA replication. Mol Cell 2005;18:425-434.
14. Naganuma A, Nozaki A, Tanaka T, Sugiyama K, Takagi H, Mori M, et al. Activation of the interferon-inducible 2′-5′-oligoadenylate synthetase gene by hepatitis C virus core protein. J Virol 2000;74:8744-8750.
15. Noguchi M, Hirohashi S. Cell lines from non-neoplastic liver and hepatocellular carcinoma tissue from a single patient. In Vitro Cell Dev Biol Anim 1996;32:135-137.
16. Dansako H, Naganuma A, Nakamura T, Ikeda F, Nozaki A, Kato N. Differential activation of interferon-inducible genes by hepatitis C virus core protein mediated by the interferon stimulated response element. Virus Res 2003;97:17-30.
17. Kato N, Sugiyama K, Namba K, Dansako H, Nakamura T, Takami M, et al. Establishment of a hepatitis C virus subgenomic replicon derived from human hepatocytes infected in vitro. Biochem Biophys Res Commun 2003;306:756-766.
18. Kocarek TA, Dahn MS, Cai H, Strom SC, Mercer-Haines NA. Regulation of CYP2B6 and CYP3A expression by hydroxymethylglutaryl coenzyme A inhibitors in primary cultured human hepatocytes. Drug Metab Dispos 2002;30:1400-1405.
19. Abe T, Kakyo M, Tokui T, Nakagomi R, Nishio T, Nakai D, et al. Identification of a novel gene family encoding human liver-specific organic anion transporter LST-1. J Biol Chem 1999;274:17159-17163.
20. Nakai D, Nakagomi R, Furuta Y, Tokui T, Abe T, Ikeda T, et al. Human liver-specific organic anion transporter, LST-1, mediates uptake of pravastatin by human hepatocytes. J Pharmacol Exp Ther 2001;297:861-867.
21. Pietschmann T, Lohmann V, Rutter G, Kurpanek K, Bartenschlager R. Characterization of cell lines carrying self-replicating hepatitis C virus RNAs. J Virol 2001;75:1252-1264.
22. Sutter AP, Maaser K, Hopfner M, Huether A, Schuppan D, Scherubl H. Cell cycle arrest and apoptosis induction in hepatocellular carcinoma cells by HMG-CoA reductase inhibitors. Synergistic antiproliferative action with ligands of the peripheral benzodiazepine receptor. J Hepatol 2005; 43:808-816.
23. Chou TC, Talalay P. Quantitative analysis of dose-effect relationships: the combined effects of multiple drugs or enzyme inhibitors. Adv Enzyme Regul 1984;22:27-55.
24. Hwang DR, Tsai YC, Lee JC, Huang KK, Lin RK, Ho CH, et al. Inhibition of hepatitis C virus replication by arsenic trioxide. Antimicrob Agents Chemother 2004;48:2876-2882.
25. Pawlotsky JM, Dahari H, Neumann AU, Hezode C, Germanidis G, Lonjon I, et al. Antiviral action of ribavirin in chronic hepatitis C. Gastroenterology 2004;126:703-714.
26. Park JW, Siekmeier R, Lattke P, Merz M, Mix C, Schuler S, et al. Pharmacokinetics and pharmacodynamics of fluvastatin in heart transplant recipients taking cyclosporine A. J Cardiovasc Pharmacol Ther 2001;6: 351-361.

Journal of General Virology (2006), 87, 1703–1713 DOI 10.1099/vir.0.81735-0

NS3 protein of *Hepatitis C virus* associates with the tumour suppressor p53 and inhibits its function in an NS3 sequence-dependent manner

Lin Deng,[1] Motoko Nagano-Fujii,[1] Motofumi Tanaka,[1,2] Yuki Nomura-Takigawa,[1] Masanori Ikeda,[3] Nobuyuki Kato,[3] Kiyonao Sada[1] and Hak Hotta[1]

Correspondence
Hak Hotta
hotta@kobe-u.ac.jp

[1,2]Divisions of Microbiology[1] and Gastroenterological Surgery[2], Kobe University Graduate School of Medicine, Kobe 650-0017, Japan

[3]Department of Molecular Biology, Okayama University Graduate School of Medicine and Dentistry, Okayama 700-8558, Japan

The N-terminal 198 residues of NS3 (NS3-N) of *Hepatitis C virus* (HCV) subtype 1b obtained from 29 patients, as well as full-length NS3 (NS3-Full), were analysed for their subcellular localization, interaction with the tumour suppressor p53 and serine protease activity in the presence and absence of the viral cofactor NS4A. Based on the subcellular-localization patterns in the absence of NS4A, NS3-N sequences were classified into three groups, with each group exhibiting either dot-like, diffuse or a mixed type of localization. Chimeric NS3-Full sequences, each consisting of an individual NS3-N and a shared C-terminal sequence, showed the same localization patterns as those of the respective NS3-N. Site-directed mutagenesis experiments revealed that a single or a few amino acid substitutions at a particular position(s) of NS3-N altered the localization pattern. Interestingly, NS3 of the dot-like type, either NS3-N or NS3-Full, interacted with p53 more strongly than that of the diffuse type, in both the presence and the absence of NS4A. Moreover, NS3-N of the dot-like type suppressed *trans*-activating activity of p53 more strongly than that of the diffuse type. Serine protease activity did not differ significantly between the two types of NS3. In HCV RNA replicon-harbouring cells, physical interaction between NS3 and p53 was observed consistently and p53-mediated transcriptional activation was suppressed significantly compared with HCV RNA-negative control cells. Our results collectively suggest the possibility that NS3 plays an important role in the hepatocarcinogenesis of HCV by interacting differentially with p53 in an NS3 sequence-dependent manner.

Received 5 December 2005
Accepted 30 January 2006

INTRODUCTION

Chronic, persistent infection with *Hepatitis C virus* (HCV) often leads to liver cirrhosis and hepatocellular carcinoma (HCC) (Saito *et al.*, 1990). However, the exact mechanisms of HCV-associated pathogenesis and carcinogenesis are largely unknown.

HCV possesses a single-stranded, positive-sense RNA genome of 9·6 kb, which encodes a polyprotein of approximately 3000 aa. The polyprotein is processed into at least 10 structural and non-structural (NS) viral proteins by cellular and viral proteases (Reed & Rice, 2000). One of the viral proteases, the NS3 serine protease, has become a research focus, as it is indispensable for virus replication and, therefore, would be a good target for antiviral drugs. The serine protease is encoded in the N-terminal portion of NS3 and is responsible for cleavage at the NS3/4A, NS4A/4B, NS4B/5A and NS5A/5B junctions. NS4A, a cofactor for NS3, stabilizes it to augment its serine protease activity, being virtually essential for complete cleavage of the HCV polyprotein (Reed & Rice, 2000). The C-terminal portion of NS3 possesses the NTPase/helicase activity (Kim *et al.*, 1995), which is essential for viral RNA replication.

In addition to its key role in the life cycle of HCV, possible involvement of NS3 in viral persistence and hepatocarcinogenesis has been studied. For example, NS3 was reported to transform NIH3T3 (Sakamuro *et al.*, 1995) and rat fibroblast (Zemel *et al.*, 2001) cells. We also demonstrated that NIH3T3 cells constitutively expressing C-terminally truncated NS3 (aa 1–433) were more resistant to actinomycin D-induced apoptosis than control cells (Fujita *et al.*, 1996). It was also reported that NS3 could block transforming growth factor-β/Smad3-mediated apoptosis (Cheng *et al.*,

Supplementary figures showing subcellular-localization patterns and a sequence alignment are available in JGV Online.

2004). Moreover, the NS3–4A complex was shown to suppress beta interferon (IFN-β) induction by inhibiting retinoic acid-inducible gene I-mediated activation of IFN regulatory factor 3, counteracting innate immune responses to help establish persistent HCV infection (Foy *et al.*, 2003, 2005; Breiman *et al.*, 2005).

The tumour-suppressor protein p53 functions principally to control cell-cycle arrest and apoptosis upon various cellular stresses, ensuring completion of DNA repair and the integrity of the genome (Levine, 1997). It has been documented that oncogenic viral proteins, such as papillomavirus E6 (Münger & Howley, 2002; Longworth & Laimins, 2004), adenovirus E1B 55K (Martin & Berk, 1998), simian virus 40 large T antigen (Sheppard *et al.*, 1999) and hepatitis B virus X protein (Truant *et al.*, 1995), inhibit p53-mediated apoptosis via interacting with p53. In the case of HCV, NS5A (Lan *et al.*, 2002) and core protein (Kao *et al.*, 2004) were reported to suppress p53-dependent apoptosis. Our previous studies showed that NS3 colocalized with p53 in the nucleus (Ishido *et al.*, 1997; Muramatsu *et al.*, 1997) and that they formed a complex through an N-terminal portion of NS3 (aa 29–174) and a C-terminal portion of p53 (Ishido & Hotta, 1998). In a clinical setting, we found a strong correlation between HCC and predicted secondary structure of an N-terminal portion of NS3 (Ogata *et al.*, 2003). These observations prompted us to investigate the possible correlation between NS3 sequence diversity and p53 interaction. We report here that subcellular localization of NS3 and its interaction with p53 vary with different NS3 sequences.

METHODS

Plasmid construction. cDNA fragments encoding the N-terminal 198 residues of NS3 (NS3-N; aa 1–198) of HCV subtype 1b (HCV-1b) isolates were described previously (Ogata *et al.*, 2002, 2003). *Bam*HI and *Hin*dIII recognition sites were introduced by PCR into the 5′ and 3′ ends of the cDNAs, respectively. The cDNAs were digested with *Bam*HI and *Hin*dIII and subcloned into pcDNA3.1/*Myc*-His(−)C (Invitrogen). A single point mutation(s) was introduced into some plasmids by using a QuikChange site-directed mutagenesis kit (Stratagene). Expression plasmids for Myc-tagged full-length NS3 (NS3-Full) of different HCV isolates, MKC1a, M-H05-5, M-45, M-H17-2 and M-42, were reported elsewhere (Hidajat *et al.*, 2005). To express NS3–4A *in cis*, the corresponding region was amplified from pTMns2-5B/810-2721 (Muramatsu *et al.*, 1997) and subcloned into pcDNA3.1/*Myc*-His(−)C to generate pcDNA3.1/MKC1a/4A. Expression plasmids for chimeric NS3-Full flanked with NS4A were constructed, in which the N-terminal 355 residues were derived from M-H05-5 or M-H17-2, whereas the C-terminal 330 residues were derived from MKC1a/4A. They were designated pcDNA3.1/M-H05-5/4A and pcDNA3.1/M-H17-2/4A. The NS3 sequences were subcloned also into pSG5 (Stratagene).

An *Eco*RI fragment encoding full-length NS4A was obtained from pBSns4A (Muramatsu *et al.*, 1997) and subcloned into pcDNA3.1/*Myc*-His(−)C and pSG5. Myc-tagged NS4A was amplified from pFK5B/2884Gly (a kind gift from Dr R. Bartenschlager, University of Heidelberg, Heidelberg, Germany) and subcloned into pEF1/*Myc*-His (Invitrogen). An expression plasmid for Myc-tagged NS4B was reported elsewhere (Tanaka *et al.*, 2006). To express a polyprotein consisting of full-length NS5A and C-terminally truncated NS5B (NS5A/5BΔC; aa 1973–2720 of the entire HCV polyprotein), the corresponding region was amplified from pTMns2-5B/810-2721 (Muramatsu *et al.*, 1997) and subcloned into pTM1 (Moss *et al.*, 1990).

An *Xho*I fragment encoding full-length wild-type p53 was obtained from pBSp53/1-393 (Ishido & Hotta, 1998) and subcloned into pcDNA3.1/*Myc*-His(−)C. pSG5/p53 (Florese *et al.*, 2002) was also used.

All of the plasmid constructs were verified for the correct sequence by DNA sequencing.

Cell culture and protein expression. Huh-7 and HeLa cells were cultured in Dulbecco's modified Eagle's medium supplemented with 10 % fetal calf serum. For protein expression, cells were infected with a recombinant vaccinia virus expressing T7 RNA polymerase (vTF7-3) (Fuerst *et al.*, 1986). After 1 h, the cells were transfected with the expression plasmids by using Lipofectin reagent (Invitrogen). After cultivation overnight, the proteins expressed in the cells were analysed by co-immunoprecipitation, immunoblot and immunofluorescence techniques, as described below. For the luciferase reporter assay, Huh-7 cells were transfected with plasmids by using Fugene 6 transfection reagent (Roche) and cultivated for 24 h before analysis.

Huh-7 cells stably harbouring an HCV subgenomic RNA replicon were prepared as described previously (Taguchi *et al.*, 2004; Hidajat *et al.*, 2005), using pFK5B/2884Gly (Lohmann *et al.*, 2001). Cured Huh-7 cells were prepared by treating the HCV replicon-harbouring cells with IFN-α (1000 IU ml^{-1}) for 1 month (Hidajat *et al.*, 2005). Full-length HCV RNA-harbouring Huh-7 cells, designated O, and IFN-cured cells, designated Oc, were described previously (Ikeda *et al.*, 2005).

Indirect immunofluorescence. Cells expressing Myc-tagged NS3 were fixed with methanol at −20 °C for 20 min and incubated with an anti-Myc mouse mAb (9E10; Santa Cruz Biotech) for 1 h at room temperature. In some experiments, an anti-NS3 mouse mAb (4A-3; a kind gift from Dr I. Fuke, Research Foundation for Microbial Diseases, Osaka University, Kagawa, Japan) was used to detect NS3-Full. An anti-haemagglutinin (HA) mouse mAb (HA.11; Covance Inc.) served as a control IgG. After being washed with PBS, the cells were incubated with fluorescein isothiocyanate-conjugated goat anti-mouse IgG (MBL) and observed under a laser-scanning confocal microscope (LSM510 version 3.0; Carl Zeiss).

Immunoprecipitation and immunoblotting. Cells expressing NS3 (Myc-tagged or untagged) and p53 were lysed in a stringent RIPA buffer containing 10 mM Tris/HCl (pH 7·5), 150 mM NaCl, 1 mM EDTA, 0·1 % SDS, 1 % NP-40, 0·1 % sodium deoxycholate and protease inhibitor cocktail (Roche) for 30 min on ice. The cell lysates were centrifuged and the supernatants were cleared by mixing with 0·25 μg normal rabbit IgG (Santa Cruz Biotech) and 15 μl protein A–Sepharose beads (Amersham Biosciences) at 4 °C for 30 min on a rotator to reduce non-specific precipitation. The cleared lysates were incubated with anti-p53 rabbit polyclonal antibody (FL-393; Santa Cruz Biotech) at 4 °C for 1 h and subsequently with 15 μl protein A–Sepharose beads for another 1 h. The beads were washed six times with RIPA buffer and the immunoprecipitates were separated by SDS-PAGE and analysed by immunoblotting (see below). To analyse the interaction of NS3 expressed in the context of HCV RNA replication with p53, the HCV subgenomic or full-length RNA replicon-harbouring cells were lysed in a mild RIPA buffer without 0·1 % SDS and 0·1 % sodium deoxycholate. The lysates were subjected to immunoprecipitation analysis in the same way as described above, except that the beads were washed with PBS instead of RIPA buffer. Anti-FLAG rabbit polyclonal antibody (Sigma) served as a control.

Immunoblot analysis was performed as described previously (Hidajat *et al.*, 2005). Mouse mAbs against Myc (9E10), NS3, NS4A (S4-13; a kind gift from Dr I. Fuke) and p53 (Ab-1; Calbiochem) were used as primary antibodies and peroxidase-labelled goat anti-mouse IgG (MBL) as a secondary antibody. The protein bands were visualized by an enhanced chemiluminescence method (ECL; Amersham Biosciences) and the intensity of the bands was quantified by using NIH Image 1.61.

Luciferase reporter assay. p53-Luc (Stratagene), which contains the *Photinus pyralis* (firefly) luciferase reporter gene driven by a basic promoter element plus an inducible *cis*-enhancer element, containing 14 repeats of the p53-binding sequence (TGCCTGGACTTGCCTGG), was used as a reporter plasmid. pRL-SV40 (Promega), which expresses *Renilla* luciferase, was used as a control plasmid to check transfection efficiency. Huh-7 cells prepared in a 24-well tissue-culture plate were transfected transiently with p53-Luc (10 ng), pRL-SV40 (1 ng), pSG5/p53 (5 ng) and pSG5/NS3-N or pSG5/NS3-Full (250 ng) in the absence or presence of pSG5/NS4A (75 ng). After 24 h, the cells were harvested and a luciferase assay was performed by using the Dual-Luciferase Reporter Assay system (Promega), as described previously (Kadoya *et al.*, 2005). Firefly and *Renilla* luciferase activities were measured by using a Luminescencer-JNR AB-2100 (Atto). Firefly luciferase activity was normalized to *Renilla* luciferase activity for each sample.

NS3 serine protease activity. HeLa cells transiently coexpressing NS5A/5BΔC and Myc-tagged NS3 were lysed in gel-loading buffer containing 50 mM Tris/HCl (pH 6·8), 5 % 2-mercaptoethanol, 2 % SDS, 0·1 % bromophenol blue and 10 % glycerol. The lysates were separated by SDS-PAGE and analysed by immunoblotting using anti-NS5A (8926; a kind gift from Dr I. Fuke) and anti-Myc antibodies (9E10). Intensity of the bands corresponding to the cleaved NS5A and the uncleaved NS5A/5BΔC was measured. Arbitrary units of serine protease activity of each NS3 were calculated by the following formula: protease activity (arbitrary units) = NS5A/(NS5A/5BΔC + NS5A).

RESULTS

NS3-N sequences of different HCV-1b isolates exhibit distinct subcellular-localization patterns in a sequence-dependent manner

We first examined the subcellular localization of NS3-N in HeLa cells. As shown in Fig. 1(a), we noticed three distinct patterns of NS3-N localization: (i) dot-like staining in both the cytoplasm and the nucleus, (ii) diffuse staining predominantly in the cytoplasm and (iii) a mixed pattern of the former two. Of the 29 HCV-1b isolates tested, 15 (52 %) exhibited exclusively the dot-like staining, nine (31 %) the diffuse staining and the remaining five (17 %) the mixed pattern. The subcellular-localization patterns of four NS3-N sequences each from the dot-like, diffuse and mixed staining groups are also shown in Supplementary Fig. S1 (available in JGV Online). Similar results were obtained when NS3-N sequences were expressed in Huh-7 cells (data not shown), suggesting that the distinct localization patterns among different NS3 sequences are not restricted to a particular cell line.

In order to see which amino acid residue(s) affected the subcellular localization of NS3, we determined the sequences of all 29 isolates. Some of the sequences showing the typical localization patterns, along with a standard sequence, are shown in Fig. 1(b). For more information, the sequences of all 29 isolates are shown in Supplementary Fig. S2 (available in JGV Online). We did not find any common amino acid residue(s) that was/were associated with a particular localization pattern. We noticed, however, that a substitution at position 17 or 18 (Ile to Val) was observed with some NS3 sequences of the dot-like pattern, but not with any NS3 sequences of the other localization patterns. Also, a substitution(s) at positions 150–153 (Val to Ala, Ile to Val) appeared to be more frequent in NS3 sequences of the dot-like pattern. To examine the possible importance of those substitutions, we introduced a point mutation(s) to some NS3-N of the dot-like pattern (Fig. 1c). Introduction of two point mutations at positions 18 and 153 into NS3-N of isolate H05-5 did not alter the localization pattern. However, introduction of an additional two point mutations at positions 80 and 122 altered the localization pattern significantly, with the majority of the cells exhibiting the typical diffuse staining. Similarly, introduction of two mutations at positions 17 and 86, but not of either one alone, into NS3-N of isolate 45 altered the localization pattern from dot-like to diffuse staining. As for isolate 63, a single point mutation at position 150 alone was enough to change the localization pattern of NS3-N. These results suggest that residues at positions 17 or 18, 80–86 and/or 150–153 play an important role in determining the localization pattern of some, but not all, NS3 sequences.

NS3-N binds to p53 and inhibits its *trans*-activating activity in an NS3 sequence-dependent manner

We previously reported that a region near the N terminus of NS3 (aa 29–174) was involved in complex formation with p53 (Ishido & Hotta, 1998). In this study, we examined whether interaction between NS3-N and p53 differs with different NS3-N sequences. We selected two NS3-N sequences each from the dot-like (H05-5 and 45) and diffuse (H17-2 and 42) staining groups. Co-immunoprecipitation analysis demonstrated that NS3-N of isolate H05-5 interacted with p53 most strongly, followed by that of isolate 45, both in the absence (Fig. 2a) and the presence (Fig. 2b) of NS4A. On the other hand, NS3-N of the diffuse-staining group interacted only weakly with p53. The specificity of the interaction between NS3-N and p53 was confirmed by a control experiment, in which neither NS4A nor NS4B bound to p53 under the same experimental conditions (Fig. 2c, left and centre panels). The specificity of the NS3–p53 interaction was also secured by another control experiment using an irrelevant (anti-FLAG) antibody (Fig. 2c, right panel).

Next, we examined the possible effect of NS3-N on p53 function. The plasmid p53-Luc harbours 14 copies of p53-responsive elements and a minimum promoter upstream of a luciferase gene, and is used to monitor p53-dependent transcriptional activity. Interestingly, NS3-N of H05-5 and that of isolate 45 inhibited p53-dependent transcription of the luciferase gene strongly and moderately, respectively

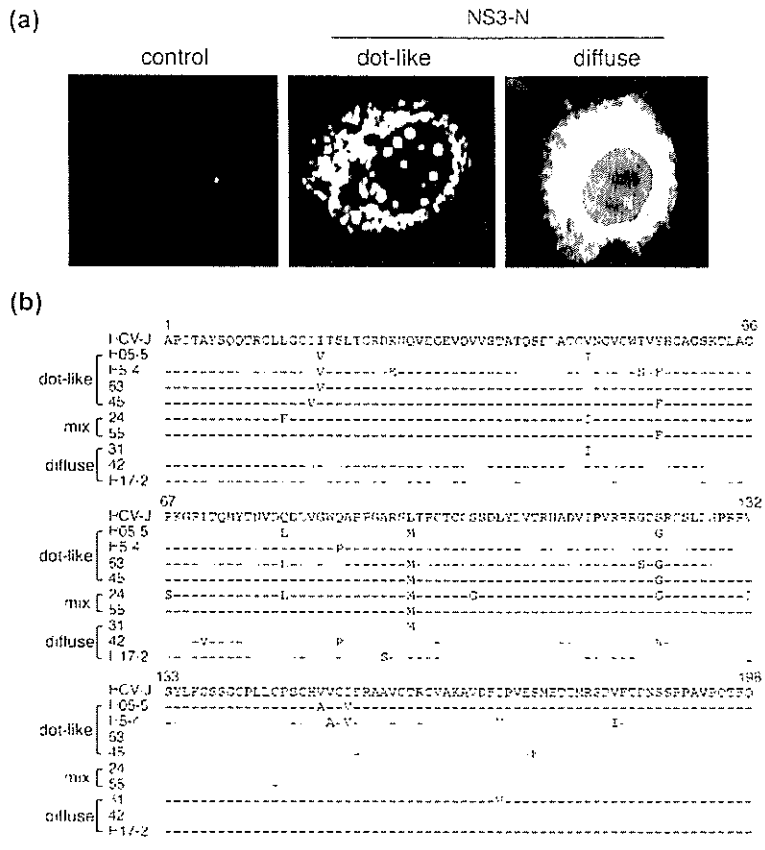

Fig. 1. Distinct subcellular-localization patterns of NS3-N of different HCV-1b isolates and the alignment of their sequences. (a) NS3-N was expressed in HeLa cells using a vaccinia virus–T7 hybrid expression method. Typical immunofluorescence images of the dot-like (middle panel) and diffuse (right panel) localization patterns of NS3-N of isolates H05-5 and H17-2, respectively, are shown. As a control, cells expressing NS3-N of H05-5 (left panel) were stained with an irrelevant (anti-HA) antibody. (b) Sequence alignment of representative sequences of each of the staining groups along with a standard sequence of the HCV-J strain (top). Dashes indicate residues identical to those of HCV-J. The numbers along the sequence indicate amino acid positions. (c) Identification of residues that alter the localization patterns of NS3-N of the isolates H05-5, 45 and 63. Substituted residues at the indicated positions are shown.

(Fig. 2d). On the other hand, no inhibition was observed with NS3-N of isolate 42 and even a slight increase in p53-dependent transcription was observed with NS3-N of H17-2.

NS3 forms a stable complex with its cofactor NS4A, which may counteract the NS3-mediated inhibitory action of p53-dependent transcription. In fact, we observed that inhibition of the p53-dependent transcription by NS3-N of the H05-5 isolate was alleviated to some extent, but not completely, by coexpression of NS4A (Fig. 2e).

To further test the possibility that the alteration in the localization pattern of NS3-N affects its interaction with p53, we compared NS3-N of H05-5 with its point mutant H05-5/mut (Fig. 1c) in terms of their p53-binding abilities and inhibitory effects on p53-dependent transcription. The result obtained demonstrated that NS3-N of H05-5/mut, which showed diffuse localization, had weaker p53-binding capacity (Fig. 3a) and exerted weaker inhibition on p53-dependent transcription (Fig. 3b) compared with NS3-N of the parental H05-5, showing the dot-like localization. Similar results were obtained with isolates 45 and 63 and their point mutants (data not shown). Our results thus suggest that NS3-N of the dot-like localization pattern interacts with p53 more strongly and inhibits p53-mediated transcriptional activation more efficiently than that of the diffuse localization.

NS3-Full sequences exhibit the same subcellular-localization patterns as those of NS3-N sequences derived from the same isolates and interact differentially with NS4A and p53 in an NS3 sequence-dependent manner

As shown above, NS3-N exhibited a distinct subcellular-localization pattern in a sequence-dependent manner when expressed alone (see Fig. 1). Moreover, we have reported that NS3, either NS3-N or NS3-Full, enters the nucleus when

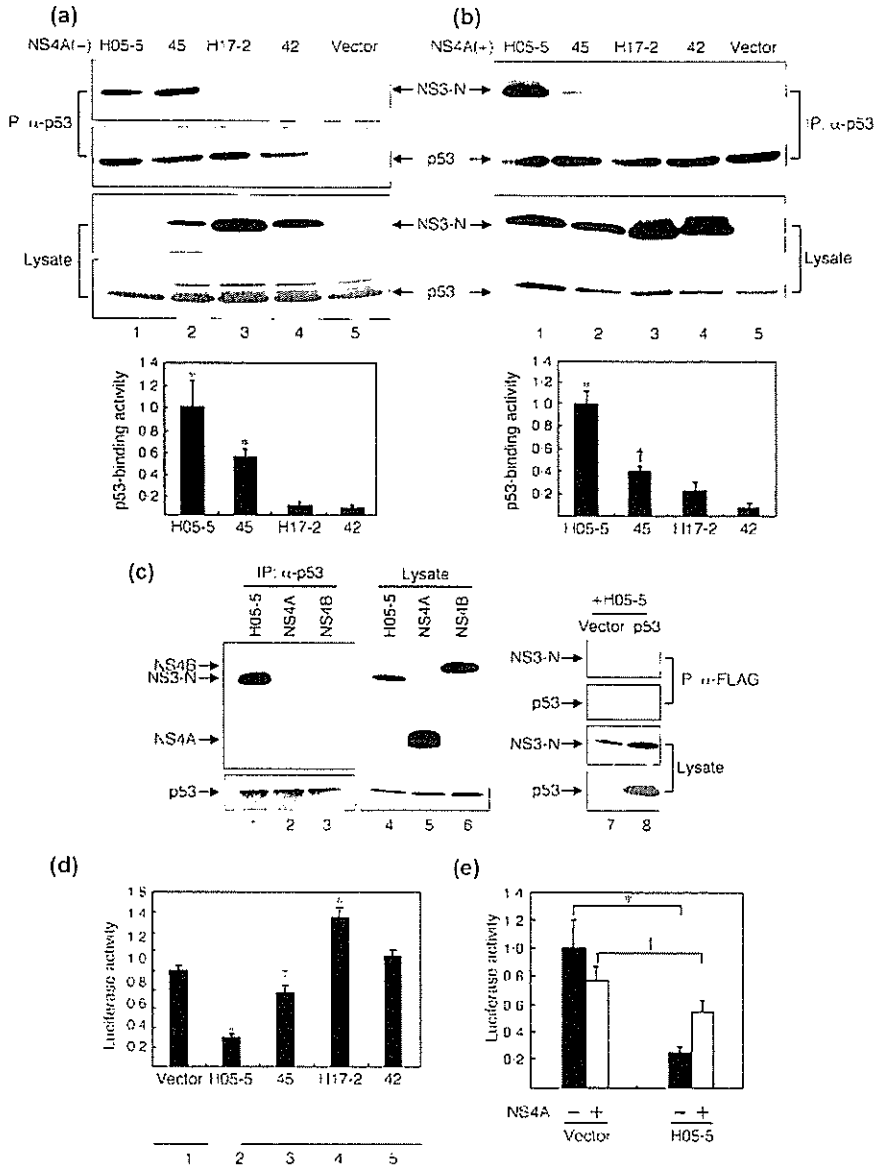

Fig. 2. Physical and functional interactions between NS3-N and p53 in an NS3 sequence-dependent manner. NS3-N and p53 were coexpressed in the absence (a) and presence (b) of NS4A. Cells that did not express NS3-N served as a control. Cell lysates were immunoprecipitated by using an anti-p53 antibody and probed by immunoblotting using an anti-Myc antibody to detect NS3-N (top row). Efficient immunoprecipitation of p53 was verified (second row). Lysates were probed directly (without being immunoprecipitated with anti-p53 antibody) with anti-Myc and anti-p53 antibodies, respectively, to verify comparable expression levels of NS3-N (third row) and p53 (bottom row). The intensity of the bands for NS3-N co-immunoprecipitated with p53 was quantified and normalized to the expression levels of NS3-N in the lysates. Filled columns and bars represent mean ± SD obtained from three independent experiments. The p53-binding intensity of NS3-N of the isolate H05-5 was expressed as 1·0. $^*P<0{\cdot}01$; $\dagger P<0{\cdot}05$, compared with isolate 42. (c) Cells expressing Myc-tagged H05-5, NS4A or NS4B together with p53 were analysed by immunoprecipitation using an anti-p53 antibody (left). Lysates were probed directly with anti-Myc and anti-p53 antibodies, respectively (middle). Cells expressing Myc-tagged H05-5 with or without p53 were analysed by immunoprecipitation using an irrelevant (anti-FLAG) antibody (right). (d) Inhibition of p53-dependent transcription by NS3-N in an NS3 sequence-dependent manner. pSG5-based NS3-N expression plasmids were each co-transfected with pSG5/p53, p53-Luc and pRL-SV40 in Huh-7 cells and cultivated for 24 h. Firefly luciferase activity was measured and normalized to *Renilla* luciferase activity. The luciferase activity in the control cells without NS3-N expression was expressed arbitrarily as 1·0. Results are shown as mean ± SD from three independent experiments. $^*P<0{\cdot}01$, $\dagger P<0{\cdot}05$, compared with the control. Expression levels of NS3-N in the cells are shown at the bottom. (e) Inhibition of p53-dependent transcription by NS3-N of H05-5 in the absence (filled bars) and presence (open bars) of NS4A. Results are shown as mean ± SD from three independent experiments. $^*P<0{\cdot}01$; $\dagger P<0{\cdot}05$, compared with the control.

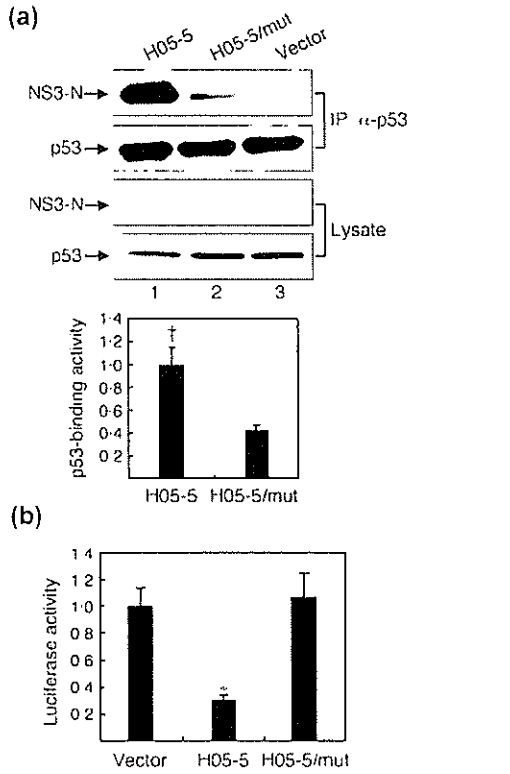

Fig. 3. Comparison between NS3-N of the isolate H05-5 and its point mutant H05-5/mut in their capacity to interact with p53. (a) Physical interaction with p53 was analysed as described in the legend to Fig. 2(a). Filled columns and bars represent mean ± SD obtained from three independent experiments. The p53-binding intensity of NS3-N of H05-5 was expressed as 1·0. †$P<0·05$. (b) Functional interaction with p53 was analysed as described in the legend to Fig. 2(c). Results are shown as mean ± SD from three independent experiments. *$P<0·01$ compared with H05-5/mut.

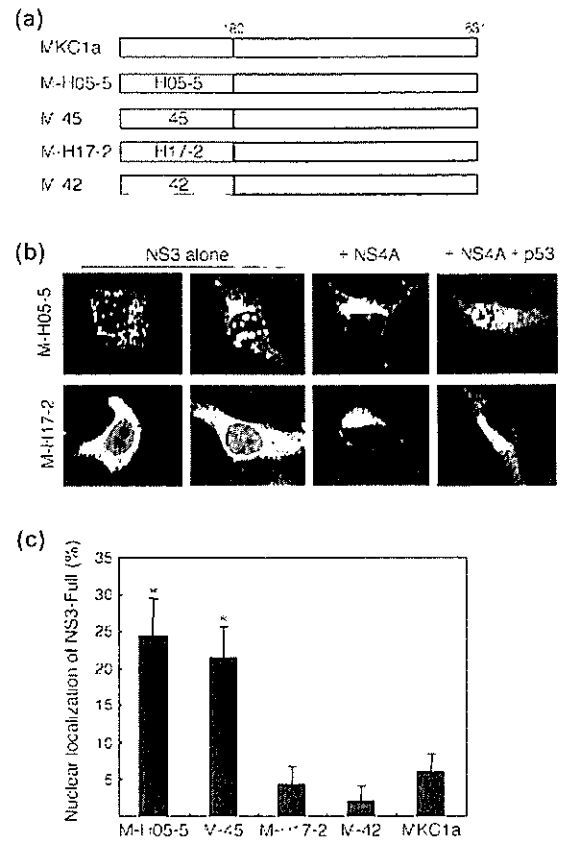

Fig. 4. Subcellular localization of NS3-Full in the presence and absence of NS4A and p53. (a) Schematic representation of NS3-Full of different sequences. The N-terminal 180 residues are derived from clinical isolates (H05-5, H17-2, 42 and 45) and the C-terminal 451 residues from the parental MKC1a strain. (b) Subcellular localization of M-H05-5 (upper) and M-H17-2 (lower) when expressed alone, when coexpressed with NS4A and when coexpressed with NS4A and p53. The cells were stained with either anti-NS3 (left panels) or anti-Myc antibody (left-middle, right-middle and right panels). (c) Percentage of cells with nuclear accumulation of NS3-Full when coexpressed with NS4A and p53. *$P<0·01$ compared with M-42.

coexpressed with p53 and that the p53-mediated nuclear localization of NS3 is inhibited by NS4A in an NS3 sequence-dependent manner (Muramatsu *et al.*, 1997). Therefore, we examined the subcellular-localization patterns of NS3-Full of different sequences, both when expressed alone and when coexpressed with p53 and/or NS4A. The NS3-Full sequences tested differ from each other only in the N-terminal 180 residues that are derived from the clinical isolates, with the C-terminal 451 residues being shared among all the strains tested (Fig. 4a; Hidajat *et al.*, 2005). When expressed alone, NS3-Full of all four strains exhibited the same subcellular-localization patterns as those of NS3-N of the same strains (Fig. 4b; data not shown for M-45 and M-42). When coexpressed with NS4A, NS3-Full was localized in the cytoplasm, especially in perinuclear regions, regardless of the strain tested. Interestingly, when p53 was additionally coexpressed with NS4A, NS3-Full of the dot-like type (M-H05-5 and M-45) showed an increased tendency to accumulate in the nucleus together with p53 (Fig. 4b), with nearly 25 % of the cells exhibiting nuclear localization of NS3 (Fig. 4c). Concomitant expression of NS4A in the cytoplasm of the same cells was confirmed by double-staining immunofluorescence analysis (data not shown), the result being consistent with our previous observation (Ishido *et al.*, 1997). On the other hand, NS3-Full of the diffuse type (M-H17-2, M-42 and MKC1a) was localized almost exclusively in the cytoplasm together with NS4A. Similar results were obtained when NS3-N sequences of different isolates were coexpressed with p53 and/or NS4A (data not shown).

We then tested complex formation between NS3-Full of the five different sequences and p53. The results demonstrated clearly that NS3-Full of the dot-like type (M-H05-5 and

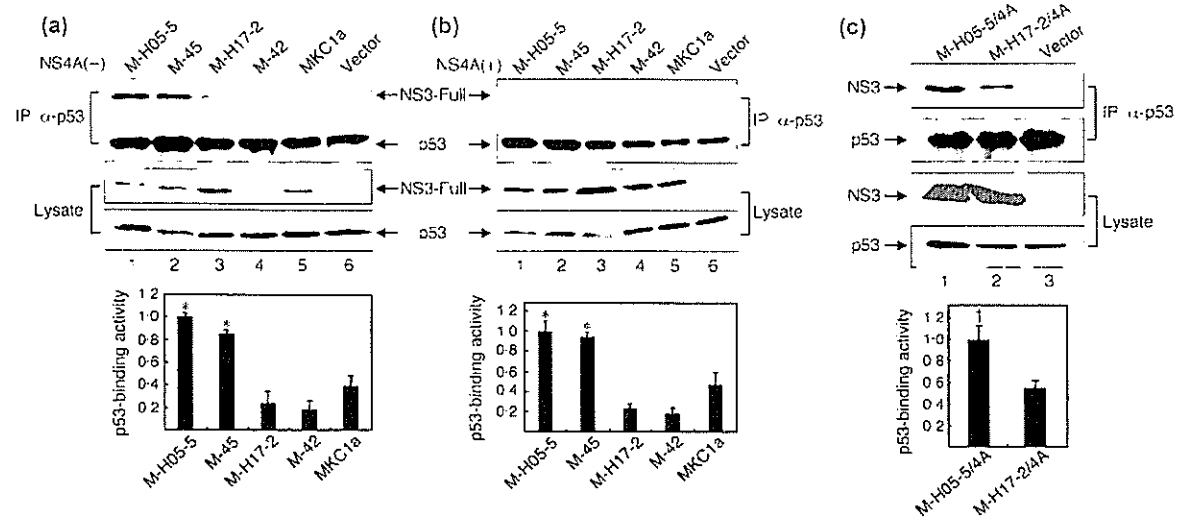

Fig. 5. Physical interaction between NS3-Full and p53 in an NS3 sequence-dependent manner. NS3-Full of different strains in the absence (a) and presence of NS4A coexpression *in trans* (b) were analysed as described in the legend to Fig. 2(a). Filled columns and bars represent mean ± SD obtained from three independent experiments. The p53-binding intensity of M-H05-5 was expressed as 1·0. *$P<0·01$ compared with M-42. (c) M-H05-5/4A and M-H17-2/4A (NS3–4A coexpression *in cis*) were analysed as described in the legend to Fig. 2(a), except that anti-NS3 antibody was used instead of anti-Myc antibody. Filled columns and bars represent mean ± SD obtained from three independent experiments. The p53-binding intensity of M-H05-5/4A was expressed as 1·0. †$P<0·05$ compared with M-H17-2/4A.

M-45) interacted with p53 more strongly than that of the diffuse type (M-H17-2, M-42 and MKC1a), both in the absence and presence of NS4A (Fig. 5a, b). In this connection, it should be noted that the interaction between NS3-Full and p53 was weaker in the presence of NS4A than in its absence. We also examined the interaction of NS3 with p53 when full-length NS3–4A was expressed *in cis*, where NS3–4A complex formation occurs more efficiently than *in trans*. The results demonstrated that M-H05-5/4A interacted with p53 more strongly than did M-H17-2/4A (Fig. 5c), again suggesting NS3 sequence-dependent interaction with p53.

NS3 binds to p53 and inhibits its *trans*-activating activity in HCV RNA replicon-harbouring cells

In order to determine whether NS3 expressed in the context of HCV replication interacted with p53, we used Huh-7 cells harbouring an HCV subgenomic RNA replicon and examined physical and functional interactions between NS3 and p53. Co-immunoprecipitation analysis revealed that NS3 interacted physically with p53 in HCV subgenomic RNA replicon-harbouring cells, albeit with much lower efficiency than in the plasmid-based expression system (Fig. 6a). We also used the full-length HCV RNA replicon, whose NS3 is detected more strongly than that of the subgenomic RNA replicon by the anti-NS3 mAb used in this study. The result demonstrated that NS3 expressed in the context of HCV RNA replication interacted efficiently with p53, irrespective of whether p53 was expressed ectopically or endogenously (Fig. 6b). The specificity of the interaction between NS3 and p53 was confirmed by the lack of interaction between NS4A and p53 in HCV subgenomic RNA-harbouring cells (Fig. 6c). Next, we compared *trans*-activating activity of p53 between HCV RNA replicon-harbouring cells and the HCV-negative controls (parental and cured Huh-7 cells). We observed that p53-dependent transcription was suppressed significantly in cells harbouring an HCV RNA replicon, either subgenomic or full-length, compared with the parental and cured Huh-7 cells (Fig. 6d, e). These results suggest collectively that NS3 expressed in the context of HCV replication inhibits p53 function.

Serine protease activity of NS3-Full in the absence and presence of NS4A

The N-terminal portion of NS3 possesses a serine protease activity that can cleave the NS5A/5B junction even in the absence of NS4A (Lin *et al.*, 1994). By using NS5A/5BΔC as a substrate, we compared the serine protease activities of NS3-Full of different subcellular-localization patterns. A tendency was noted that, in the absence of NS4A, NS3-Full of the dot-like type showed slightly weaker protease activity than that of the diffuse type (Fig. 7). This difference might be attributable, at least partly, to the fact that NS5A/5BΔC was localized diffusely in the cytoplasm (Kim *et al.*, 1999; Mottola *et al.*, 2002; data not shown) and, therefore, could be recognized more easily by NS3 of the same localization pattern than by NS3 of the other type. In the presence of

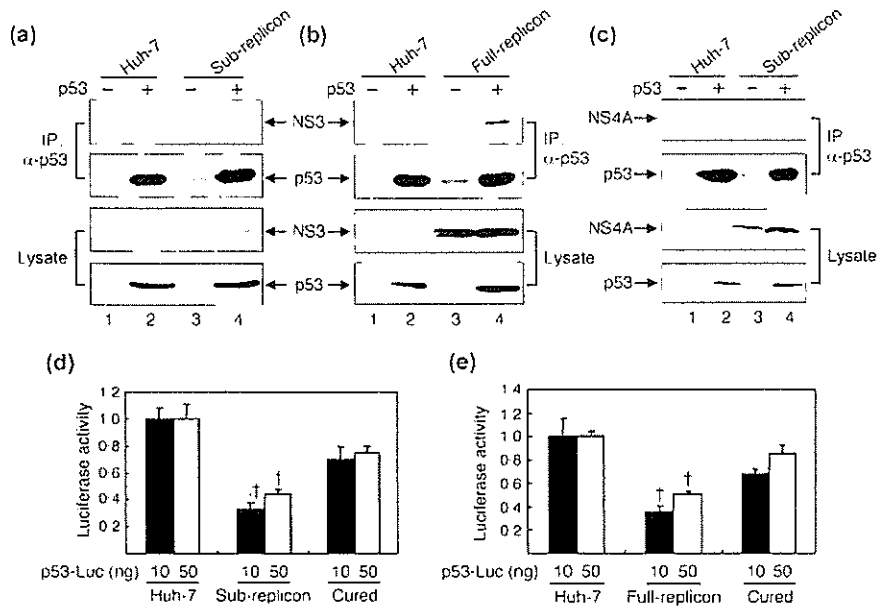

Fig. 6. Physical and functional interactions between NS3 and p53 in HCV RNA replicon-harbouring cells. p53 was expressed ectopically in Huh-7 cells harbouring either HCV subgenomic (a) or full-length (b) RNA replicon and the parental Huh-7 cells by using a vaccinia virus–T7 hybrid expression method. Cell lysates were analysed as described in Methods. (c) The lack of interaction between NS4A and p53 in HCV subgenomic RNA replicon-harbouring Huh-7 cells was confirmed. Inhibition of p53-dependent transcription in Huh-7 cells harbouring either HCV subgenomic (d) or full-length (e) RNA replicon. Cells were co-transfected with p53-Luc (10 and 50 ng, filled and open bars, respectively), pSG5/p53 (10 ng) and pRL-SV40 (1 ng) as an internal control. After 24 h, firefly luciferase activity was measured and normalized to *Renilla* luciferase activity. Luciferase activities in the parental Huh-7 cells were expressed arbitrarily as 1·0. Cured cells also served as a control. Results are shown as mean ± SD from three independent experiments. $^{*}P<0{\cdot}01$; $\dagger P<0{\cdot}05$, compared with the parental and cured Huh-7 cells.

NS4A, on the other hand, all of the NS3-Full sequences, which accumulated at a perinuclear region of the cytoplasm (see Fig. 4b), exhibited an enhanced and comparable degree of serine protease activity among the five strains (Fig. 7). Similar results were obtained when Huh-7 cells were used instead of HeLa cells (data not shown).

DISCUSSION

In the present study we demonstrated that, when expressed alone, NS3 of HCV-1b isolates, either NS3-N or NS3-Full, exhibited distinct subcellular-localization patterns, i.e. (i) dot-like staining both in the cytoplasm and the nucleus, (ii) diffuse staining predominantly in the cytoplasm and (iii) a mixed type, in a sequence-dependent manner (Figs 1 and 4). Although no significant correlation has been observed so far between the localization patterns of NS3 and the HCC status of the patients, it was interesting to find that NS3-N and NS3-Full of the dot-like staining pattern interacted with p53 more strongly than that of the diffuse-staining pattern (Figs 2a, 3a and 5a). Similar results were obtained when NS3 was coexpressed with NS4A (Figs 2b, 5b and 5c). We also observed that both NS3-N and NS3-Full of the dot-like staining pattern, but not those of the diffuse pattern, were more prone to colocalize with p53 in the nucleus even in the presence of NS4A (Fig. 4). Luciferase reporter analysis demonstrated that NS3-N of the dot-like type, but not that of the diffuse type, suppressed p53-dependent transcriptional activation significantly (Figs 2d and 3b).

When cells are exposed to a variety of stresses, p53 is induced to accumulate in the nucleus, where it functions as a transcription factor for cell-cycle regulators such as p21 (Levine, 1997). Our present results demonstrated that NS3-N of isolate H05-5 inhibited p53-dependent transcription of a reporter gene strongly (Figs 2d and 3b). We need to assess two possible mechanisms for the NS3-N-mediated p53 inhibition: NS3 might inhibit either p53 expression or p53 function itself. Our results showed that p53 expression levels were not altered significantly by NS3-N, irrespective of the localization patterns (Fig. 2a, b, bottom). Similar results that neither p53 mRNA nor protein levels were downregulated by NS3 were reported by Kwun *et al.* (2001). Overexpression of p53 was even observed in hepatocytes of some, if not all, HCV-infected patients (Loguercio *et al.*, 2003). It is likely, therefore, that NS3-N inhibits p53 function by interacting with it physically.

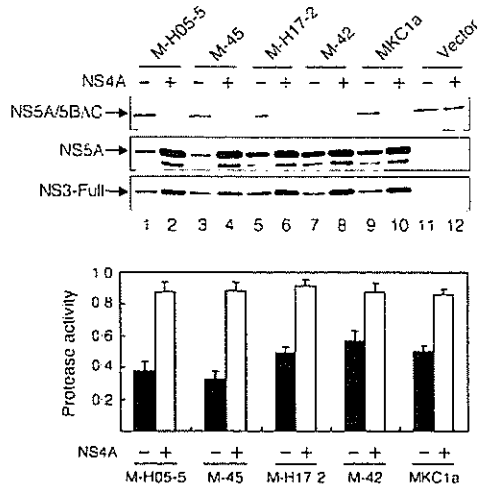

Fig. 7. Serine protease activity of NS3-Full in the absence and presence of NS4A. NS3-Full of different strains and NS5A/5BΔC were coexpressed in HeLa cells without (lanes with odd numbers) or with (lanes with even numbers) NS4A using a vaccinia virus–T7 hybrid expression method. Cell lysates were subjected to immunoblotting using anti-NS5A or anti-Myc antibody to detect NS5A/5BΔC (top), NS5A (middle) and NS3 (bottom). The intensity of the bands was quantified and arbitrary units of serine protease activity were calculated as described in Methods. Serine protease activities of NS3-Full in the absence (filled bars) and presence (open bars) of NS4A obtained from three independent experiments are shown.

We previously reported that a region of p53 near the C terminus (aa 301–360) was involved in complex formation with NS3 (Ishido & Hotta, 1998). This region includes the p53 oligomerization domain (aa 324–355) (Levine, 1997). It is known that the p53 tetramer binds to the p53-response element on promoter sequences most efficiently and, therefore, is most effective in *trans*-activation of its target genes (McLure & Lee, 1998; Weinberg *et al.*, 2004). Recently, it was reported that proteins of the S100 family disrupted p53 tetramerization via binding to its tetramerization domain (Fernandez-Fernandez *et al.*, 2005). Therefore, it is reasonable to assume that interaction of NS3-N with p53 interferes with its tetramer formation and DNA binding, thereby inhibiting p53-dependent transcriptional activation. It was also reported that a C-terminal portion of p53 (aa 364–393) negatively regulated its DNA-binding capacity (Müller-Tiemann *et al.*, 1998) and that the 14-3-3 proteins could associate with this region to counteract the negative regulation, which resulted in increased DNA binding of p53 (Waterman *et al.*, 1998). It is tempting to speculate that, by binding to a nearby region of p53, NS3-N may impair the association of 14-3-3 proteins with p53, which results in comparably decreased DNA binding of p53. Moreover, p53 is subject to post-translational modifications, including phosphorylation and acetylation, that affect p53 function (Appella & Anderson, 2001). Further study is needed to determine whether such p53 modification status is affected, either directly or indirectly, by NS3-N.

Consistent with the results obtained from transient-expression experiments, physical interaction between NS3 and p53 was also observed in Huh-7 cells harbouring either an HCV subgenomic or full-length RNA replicon, albeit to a smaller extent than in the transient-expression system (Fig. 6). It should be noted that NS3 expressed by the full-length RNA replicon is detected more strongly by the anti-NS3 antibody used in this study than that of the subgenomic RNA replicon. In HCV RNA replicon-harbouring cells, the HCV non-structural proteins are incorporated into the HCV RNA replication complex and, therefore, it is conceivable that only a minor fraction of NS3 is available for the interaction with p53. Nevertheless, p53-mediated transcriptional activation was suppressed significantly in HCV RNA replicon-harbouring cells compared with the controls (Fig. 6d, e). We must consider the possibility that not only NS3, but also other HCV proteins, are involved in the observed p53 inhibition. In fact, interaction between NS5A and p53 has been reported (Lan *et al.*, 2002; Qadri *et al.*, 2002).

In conclusion, our present results have demonstrated that NS3 of HCV-1b can be divided into three groups based on the subcellular-localization patterns and that NS3 of the dot-like localization pattern interacts with, and inhibits the function of, the tumour suppressor p53 more strongly than that of the diffuse type. The observed difference may account, at least partly, for a different degree of the oncogenic capacity of different HCV-1b isolates.

ACKNOWLEDGEMENTS

The authors are grateful to Dr I. Fuke, Research Institute for Microbial Diseases, Kan-Onji Branch, Kagawa, Japan, for providing anti-NS3, anti-NS4A and anti-NS5A mAbs. Thanks are also due to Dr R. Bartenschlager (University of Heidelberg, Heidelberg, Germany) for providing an HCV subgenomic RNA replicon (pFK5B/2884Gly). This study was supported in part by Grants-in-Aid for Scientific Research from the Ministry of Education, Culture, Sports, Science and Technology, the Japan Society for the Promotion of Science and the Ministry of Health, Labour and Welfare, Japan. This study was also carried out as part of the 21COE Program at Kobe University Graduate School of Medicine.

REFERENCES

Appella, E. & Anderson, C. W. (2001). Post-translational modifications and activation of p53 by genotoxic stresses. *Eur J Biochem* 268, 2764–2772.

Breiman, A., Grandvaux, N., Lin, R., Ottone, C., Akira, S., Yoneyama, M., Fujita, T., Hiscott, J. & Meurs, E. F. (2005). Inhibition of RIG-I-dependent signaling to the interferon pathway during hepatitis C virus expression and restoration of signaling by IKKε. *J Virol* 79, 3969–3978.

Cheng, P.-L., Chang, M.-H., Chao, C.-H. & Wu Lee, Y.-H. (2004). Hepatitis C viral proteins interact with Smad3 and differentially regulate TGF-β/Smad3-mediated transcriptional activation. *Oncogene* 23, 7821–7838.

Fernandez-Fernandez, M. R., Veprintsev, D. B. & Fersht, A. R. (2005). Proteins of the S100 family regulate the oligomerization of p53 tumor suppressor. *Proc Natl Acad Sci U S A* 102, 4735–4740.

Florese, R. H., Nagano-Fujii, M., Iwanaga, Y., Hidajat, R. & Hotta, H. (2002). Inhibition of protein synthesis by the nonstructural proteins NS4A and NS4B of hepatitis C virus. *Virus Res* 90, 119–131.

Foy, E., Li, K., Wang, C., Sumpter, R., Jr, Ikeda, M., Lemon, S. M. & Gale, M., Jr (2003). Regulation of interferon regulatory factor-3 by the hepatitis C virus serine protease. *Science* 300, 1145–1148.

Foy, E., Li, K., Sumpter, R., Jr & 8 other authors (2005). Control of antiviral defenses through hepatitis C virus disruption of retinoic acid-inducible gene-I signaling. *Proc Natl Acad Sci U S A* 102, 2986–2991.

Fuerst, T. R., Niles, E. G., Studier, F. W. & Moss, B. (1986). Eukaryotic transient-expression system based on recombinant vaccinia virus that synthesizes bacteriophage T7 RNA polymerase. *Proc Natl Acad Sci U S A* 83, 8122–8126.

Fujita, T., Ishido, S., Muramatsu, S., Itoh, M. & Hotta, H. (1996). Suppression of actinomycin D-induced apoptosis by the NS3 protein of hepatitis C virus. *Biochem Biophys Res Commun* 229, 825–831.

Hidajat, R., Nagano-Fujii, M., Deng, L., Tanaka, M., Takigawa, Y., Kitazawa, S. & Hotta, H. (2005). Hepatitis C virus NS3 protein interacts with ELKS-δ and ELKS-α, members of a novel protein family involved in intracellular transport and secretory pathways. *J Gen Virol* 86, 2197–2208.

Ikeda, M., Abe, K., Dansako, H., Nakamura, T., Naka, K. & Kato, N. (2005). Efficient replication of a full-length hepatitis C virus genome, strain O, in cell culture, and development of a luciferase reporter system. *Biochem Biophys Res Commun* 329, 1350–1359.

Ishido, S. & Hotta, H. (1998). Complex formation of the non-structural protein 3 of hepatitis C virus with the p53 tumor suppressor. *FEBS Lett* 438, 258–262.

Ishido, S., Muramatsu, S., Fujita, T., Iwanaga, Y., Tong, W.-Y., Katayama, Y., Itoh, M. & Hotta, H. (1997). Wild-type, but not mutant-type, p53 enhances nuclear accumulation of the NS3 protein of hepatitis C virus. *Biochem Biophys Res Commun* 230, 431–436.

Kadoya, H., Nagano-Fujii, M., Deng, L., Nakazono, N. & Hotta, H. (2005). Nonstructural proteins 4A and 4B of hepatitis C virus transactivate the interleukin 8 promoter. *Microbiol Immunol* 49, 265–273.

Kao, C.-F., Chen, S.-Y., Chen, J.-Y. & Wu Lee, Y.-H. (2004). Modulation of p53 transcription regulatory activity and post-translational modification by hepatitis C virus core protein. *Oncogene* 23, 2472–2483.

Kim, D. W., Gwack, Y., Han, J. H. & Choe, J. (1995). C-terminal domain of the hepatitis C virus NS3 protein contains an RNA helicase activity. *Biochem Biophys Res Commun* 215, 160–166.

Kim, J.-E., Song, W. K., Chung, K. M., Back, S. H. & Jang, S. K. (1999). Subcellular localization of hepatitis C viral proteins in mammalian cells. *Arch Virol* 144, 329–343.

Kwun, H. J., Jung, E. Y., Ahn, J. Y., Lee, M. N. & Jang, K. L. (2001). p53-dependent transcriptional repression of $p21^{waf1}$ by hepatitis C virus NS3. *J Gen Virol* 82, 2235–2241.

Lan, K.-H., Sheu, M.-L., Hwang, S.-J. & 8 other authors (2002). HCV NS5A interacts with p53 and inhibits p53-mediated apoptosis. *Oncogene* 21, 4801–4811.

Levine, A. J. (1997). p53, the cellular gatekeeper for growth and division. *Cell* 88, 323–331.

Lin, C., Prágai, B. M., Grakoui, A., Xu, J. & Rice, C. M. (1994). Hepatitis C virus NS3 serine proteinase: *trans*-cleavage requirements and processing kinetics. *J Virol* 68, 8147–8157.

Loguercio, C., Cuomo, A., Tuccillo, C., Gazzerro, P., Cioffi, M., Molinari, A. M. & Del Vecchio Blanco, C. (2003). Liver p53 expression in patients with HCV-related chronic hepatitis. *J Viral Hepat* 10, 266–270.

Lohmann, V., Körner, F., Dobierzewska, A. & Bartenschlager, R. (2001). Mutations in hepatitis C virus RNAs conferring cell culture adaptation. *J Virol* 75, 1437–1449.

Longworth, M. S. & Laimins, L. A. (2004). Pathogenesis of human papillomaviruses in differentiating epithelia. *Microbiol Mol Biol Rev* 68, 362–372.

Martin, M. E. D. & Berk, A. J. (1998). Adenovirus E1B 55K represses p53 activation in vitro. *J Virol* 72, 3146–3154.

McLure, K. G. & Lee, P. W. K. (1998). How p53 binds DNA as a tetramer. *EMBO J* 17, 3342–3350.

Moss, B., Elroy-Stein, O., Mizukami, T., Alexander, W. A. & Fuerst, T. R. (1990). New mammalian expression vectors. *Nature* 348, 91–92.

Mottola, G., Cardinali, G., Ceccacci, A., Trozzi, C., Bartholomew, L., Torrisi, M. R., Pedrazzini, E., Bonatti, S. & Migliaccio, G. (2002). Hepatitis C virus nonstructural proteins are localized in a modified endoplasmic reticulum of cells expressing viral subgenomic replicons. *Virology* 293, 31–43.

Müller-Tiemann, B. F., Halazonetis, T. D. & Elting, J. J. (1998). Identification of an additional negative regulatory region for p53 sequence-specific DNA binding. *Proc Natl Acad Sci U S A* 95, 6079–6084.

Münger, K. & Howley, P. M. (2002). Human papillomavirus immortalization and transformation functions. *Virus Res* 89, 213–228.

Muramatsu, S., Ishido, S., Fujita, T., Itoh, M. & Hotta, H. (1997). Nuclear localization of the NS3 protein of hepatitis C virus and factors affecting the localization. *J Virol* 71, 4954–4961.

Ogata, S., Ku, Y., Yoon, S., Makino, S., Nagano-Fujii, M. & Hotta, H. (2002). Correlation between secondary structure of an amino-terminal portion of the nonstructural proteins 3 (NS3) of hepatitis C virus and development of hepatocellular carcinoma. *Microbiol Immunol* 46, 549–554.

Ogata, S., Florese, R. H., Nagano-Fujii, M. & 7 other authors (2003). Identification of hepatitis C virus (HCV) subtype 1b strains that are highly, or only weakly, associated with hepatocellular carcinoma on the basis of the secondary structure of an amino-terminal portion of the HCV NS3 protein. *J Clin Microbiol* 41, 2835–2841.

Qadri, I., Iwahashi, M. & Simon, F. (2002). Hepatitis C virus NS5A protein binds TBP and p53, inhibiting their DNA binding and p53 interactions with TBP and ERCC3. *Biochim Biophys Acta* 1592, 193–204.

Reed, K. E. & Rice, C. M. (2000). Overview of hepatitis C virus genome structure, polyprotein processing, and protein properties. *Curr Top Microbiol Immunol* 242, 55–84.

Saito, I., Miyamura, T., Ohbayashi, A. & 10 other authors (1990). Hepatitis C virus infection is associated with the development of hepatocellular carcinoma. *Proc Natl Acad Sci U S A* 87, 6547–6549.

Sakamuro, D., Furukawa, T. & Takegami, T. (1995). Hepatitis C virus nonstructural protein NS3 transforms NIH3T3 cells. *J Virol* 69, 3893–3896.

Sheppard, H. M., Corneillie, S. I., Espiritu, C., Gatti, A. & Liu, X. (1999). New insights into the mechanism of inhibition of p53 by simian virus 40 large T antigen. *Mol Cell Biol* 19, 2746–2753.

Taguchi, T., Nagano-Fujii, M., Akutsu, M., Kadoya, H., Ohgimoto, S., Ishido, S. & Hotta, H. (2004). Hepatitis C virus NS5A protein interacts with 2′,5′-oligoadenylate synthetase and inhibits antiviral activity of IFN in an IFN sensitivity-determining region-independent manner *J Gen Virol* 85, 959–969.

Tanaka, M., Nagano-Fujii, M., Deng, L., Ishido, S., Sada, K. & Hotta, H. (2006). Single-point mutations of hepatitis C virus NS3 that impair p53 interaction and anti-apoptotic activity of NS3. *Biochem Biophys Res Commun* 340, 792–799.

Truant, R., Antunovic, J., Greenblatt, J., Prives, C. & Cromlish, J. A. (1995). Direct interaction of the hepatitis B virus HBx protein with p53 leads to inhibition by HBx of p53 response element directed-transactivation. *J Virol* 69, 1851–1859.

Waterman, M. J. F., Stavridi, E. S., Waterman, J. L. F. & Halazonetis, T. D. (1998). ATM-dependent activation of p53 involves dephosphorylation and association with 14-3-3 proteins. *Nat Genet* 19, 175–178.

Weinberg, R. L., Veprintsev, D. B. & Fersht, A. R. (2004). Cooperative binding of tetrameric p53 to DNA. *J Mol Biol* 341, 1145–1159.

Zemel, R., Gerechet, S., Greif, H. & 7 other authors (2001). Cell transformation induced by hepatitis C virus NS3 serine protease. *J Viral Hepat* 8, 96–102.

Available online at www.sciencedirect.com
SCIENCE DIRECT®
Virology 346 (2006) 348 – 362
VIROLOGY
www.elsevier.com/locate/yviro

Hepatitis C virus NS5B delays cell cycle progression by inducing interferon-β via Toll-like receptor 3 signaling pathway without replicating viral genomes

Kazuhito Naka [a,1], Hiromichi Dansako [a,1], Naoya Kobayashi [b], Masanori Ikeda [a], Nobuyuki Kato [a,*]

[a] *Department of Molecular Biology, Okayama University Graduate School of Medicine, Dentistry, and Pharmaceutical Sciences, 2-5-1 Shikata-cho, Okayama 700-8558, Japan*
[b] *Department of Surgery, Okayama University Graduate School of Medicine, Dentistry, and Pharmaceutical Sciences, 2-5-1 Shikata-cho, Okayama 700-8558, Japan*

Received 1 July 2005; returned to author for revision 11 August 2005; accepted 18 October 2005
Available online 2 December 2005

Abstract

To clarify the pathogenesis of hepatitis C virus (HCV), we have studied the effects of HCV proteins using human hepatocytes. Here, we found that HCV NS5B, an RNA-dependent RNA polymerase, delayed cell cycle progression through the S phase in PH5CH8 immortalized human hepatocyte cells. Since treatment with anti-interferon (IFN)-β neutralizing antibody restored the cell cycle delay, IFN-β was deemed responsible for the cell cycle delay in NS5B-expressing PH5CH8 cells. The induction of IFN-β and the cell cycle delay were overridden by the down-regulation of Toll-like receptor 3 (TLR3) through RNA interference in NS5B-expressing PH5CH8 cells. Moreover, the NS5B full form was required for the cell cycle delay, the induction of IFN-β, and the activation of the IFN-β signaling pathway. Our findings revealed that NS5B induced IFN-β through the TLR3 signaling pathway in immortalized human hepatocytes even without replicating viral genomes.

Keywords: Hepatitis C virus; NS5B; Interferon-β; TLR3; Hepatocyte cells

Introduction

Since more than 170 million individuals are estimated to be infected with hepatitis C virus (HCV) worldwide, this disease is a global health problem (Thomas, 2000). HCV belongs to the family Flaviviridae, whose positive-stranded RNA genome encodes a large polyprotein precursor of approximately 3000 amino acid residues. This polyprotein is processed by a combination of the host and viral proteases into at least ten proteins in the following order: NH_2-core-envelope 1-envelope 2-p7-nonstructural protein 2 (NS2)-NS3-NS4A-NS4B-NS5A-NS5B-COOH (Kato, 2001; Kato et al., 1990). These viral proteins are not only involved in viral replication but also may affect a variety of cellular functions (Bartenschlager and Lohmann, 2000; Kato, 200). Although persistent infection with HCV is a major cause of chronic hepatitis, liver cirrhosis, and hepatocellular carcinoma (HCC) (Colombo, 1996; Kato, 2001), the molecular mechanisms leading to liver cell dysplasia and HCC remain elusive.

It has been thought that unregulated cell cycle progression may be a cause of malignant transformation of normal cells. On the other hand, inhibition of cell cycle progression through the S phase may cause replication error during DNA replication, which induces genomic instability and malignant transformation. Therefore, it is important to clarify the effect of HCV proteins on cell cycle progression in order to understand the molecular mechanism underlying the pathogenesis of HCV, including the development of HCC. A number of previous reports suggested that four HCV proteins—the core, NS3, NS4B, and NS5A—are involved in modulating cell cycle progression (200 , Ra and Ray 200 Reed and Rice, 2000). For instance, the core protein promotes cell proliferation through the Ras/Raf signaling pathway and the anti-apoptotic function (Mar-

* Corresponding author. Fax: +81 86 235 7392.
E-mail address: nkato@md.okaya ic. (N. Kato).
[1] Both authors contributed equally to this work.

0042-6822/$ - see front matter © 2005 Elsevier Inc. All rights reserved.
doi:10.1016/j.virol.2005.10.023

usawa et al., 1999; Tsuchihara et al., 1999). However, the core has been described to both enhance and repress the function of $p21^{Waf1/Cip1/Sdi1}$, a Cdk inhibitor (Dubourdeau et al., 2002; Jung et al., 2001; Lu et al., 1999; Ray et al., 1998). Recently, Scholle et al. found no significant cell cycle delay in human hepatoma HuH-7-based HCV RNA-replicating cells that were autonomously replicating genome-length HCV RNA, in comparison with cured cells of the same line from which HCV RNA had been eliminated by treatment with interferon (IFN)-α (Scholle et al., 2004). Hence, the effects of cell cycle regulation by HCV proteins are still controversial. Cancerous cell lines, such as the human hepatoma HuH-7 cell line (Hsu et al., 1993), which harbors a mutant *p53* gene, may not be suitable for addressing the effects of HCV proteins on cell cycle progression.

The PH5CH8 cell line was established by immortalization using the SV40 large-T antigen from non-neoplastic liver tissue of an HCV-related HCC patient (Ikeda et al., 1998; Noguchi and Hirohashi, 1996). PH5CH8 cells possess wild-type *p53* and *Rb* tumor suppressor genes. In nude mice, these cells reveal a non-malignant phenotype upon colony formation and tumorigenicity (Noguchi and Hirohashi, 1996), although the SV40 large-T antigen would partially repress the function of p53. Therefore, the PH5CH8 cell line is considered to be more relevant for studying the role of HCV proteins during hepatocarcinogenesis. We have previously reported that the HCV core protein activates the IFN-inducible 2′–5′-oligoadenylate synthetase gene in PH5CH8 cells (Naganuma et al., 2000). Recently, we demonstrated that the core protein's activation of this gene was mediated through the IFN-stimulated response element (ISRE) (Dansako et al., 2003). Furthermore, we found that the core protein promoted microsatellite instability in PH5CH8 cells (Naganuma et al., 2004). In fact, microsatellite instability was detected in approximately 20% of the tumor tissues from HCC patients examined, whereas no microsatellite instability was detected in normal liver tissues from the same patients (Dore et al., 2001, Kondo et al., 2000). In order to clarify the effect of HCV proteins on cell cycle progression in PH5CH8 cells, we examined cell cycle progression after the cells were released from the G1/S boundary in PH5CH8 cells expressing HCV proteins. We found that NS5B delays cell cycle progression by inducing IFN-β through the activation of the Toll-like receptor 3 (TLR3) signaling pathway without replicating viral genomes.

Results

HCV NS5B causes the delay of S phase progression

In a previous study of virus–host interactions, we examined whether or not HCV proteins affect cell cycle progression in PH5CH8 cells that stably expressed core or NS proteins. PH5CH8 cells were infected with retrovirus pCXbsr as a negative control (Ctr) or pCXbsr encoding either an HCV structural protein (HA-core) or NS protein (NS3, HA-NS4B, HA-NS5A, HA-NS5B, or NS5B), and we obtained PH5CH8 cells stably expressing each HCV protein. The expression of each HCV protein was confirmed by Western blot analysis (Fig. 1A). Then, the HCV protein-expressing cells were synchronized at the G1/S boundary, and cell cycle progression (from the S phase to the G2-M phase, then turning back to the G1 phase) was analyzed after the cells were released from synchronization. This cell cycle analysis revealed no significant differences in cell cycle progression between cells (PH/Ctr) infected with a control pCXbsr retrovirus and cells expressing core, NS3, NS4B, or NS5A (Fig. 1B). Unlike the PH/Ctr cells, the apparent delay of S phase progression was found in cells (PH/NS5B) expressing NS5B, regardless of the presence of the HA tag (Fig. 1B). To exclude the possibility that pCXbsr-derived retrovirus proteins synergistically affect the cell cycle together with NS5B, the retrovirus pCX4bsr vector (Akagi et al., 2003), which eliminates the production of any fusion proteins resulting from initiation at upstream AUG codons within the *gag* region of the vector, was used for the cell cycle analysis. As a result, the delay of S phase progression was found again in PH5CH8 cells expressing NS5B (Figs. 1A and C), suggesting that the retrovirus proteins are not involved in the delay of S phase progression. BrdUrd incorporation analysis was also carried out using PH/Ctr and PH/NS5B cells (Fig. 1D). In the PH/Ctr cells, DNA synthesis began early in the S phase (4 h after release). In the late S phase (8 h), more than 61% of the cells indicated final DNA synthesis. Thereafter, the cells either finished DNA replication in the G2-M phase (12 h) or returned to the G1 phase. In contrast, we found that DNA replication in most PH/NS5B cells predominantly remained in the early or middle S phase (8 h), and 49% of the cells were prolonged in the late S phase (12 h). To quantitatively evaluate this delay in S phase progression, the cells that had finished DNA replication were accumulated during the G2 phase by treatment with Nocodazole (Noc), which inhibits the progression of the G2 to M phases, after the cells were released from the G1/S transition. Whereas 77% of PH/Ctr cells reached the G2-M phase, only 37% of PH/NS5B cells did so (Fig. 1D). This level of decrease in cell numbers in the G2-M phase was not observed in PH5CH8 cells expressing core, NS3, NS4B, or NS5A (Fig. 1E), suggesting that NS5B specifically causes the delay of S phase progression in PH5CH8 cells. We further observed that the growth rate of PH/NS5B cells was significantly decreased relative to PH/Ctr cells (Fig. 1F), although the cell cycle distribution in asynchronous PH/NS5B cells was almost the same as that in asynchronous PH/Ctr cells (Fig. 1D). These results indicated that NS5B might delay the cell cycle progression of PH5CH8 cells in the S phase.

Cell cycle delay by NS5B is also found in other immortalized human hepatocytes

To clarify whether or not the delay of S phase progression by NS5B occurs in other human cell lines, we prepared three cell lines (Fig. 2A) that stably express NS5B–non-neoplastic human hepatocyte NKNT-3 (Kobayashi et al. 2000), hepatoma

HuH-7, and cervical carcinoma HeLa—and subjected them to the cell cycle analysis described above. The results revealed that S phase progression was delayed in NKNT-3, but not in HuH-7 or HeLa cells (Fig. 2B). This indicates that the delay of the cell cycle by NS5B expression is not limited to PH5CH8 cells.

IFN-β mediates the delay of S phase progression by NS5B

Since it has been reported previously that IFN-β induced the delay of S phase progression in human cultured cells (Vannucchi et al., 2000), we speculated that IFN-β was

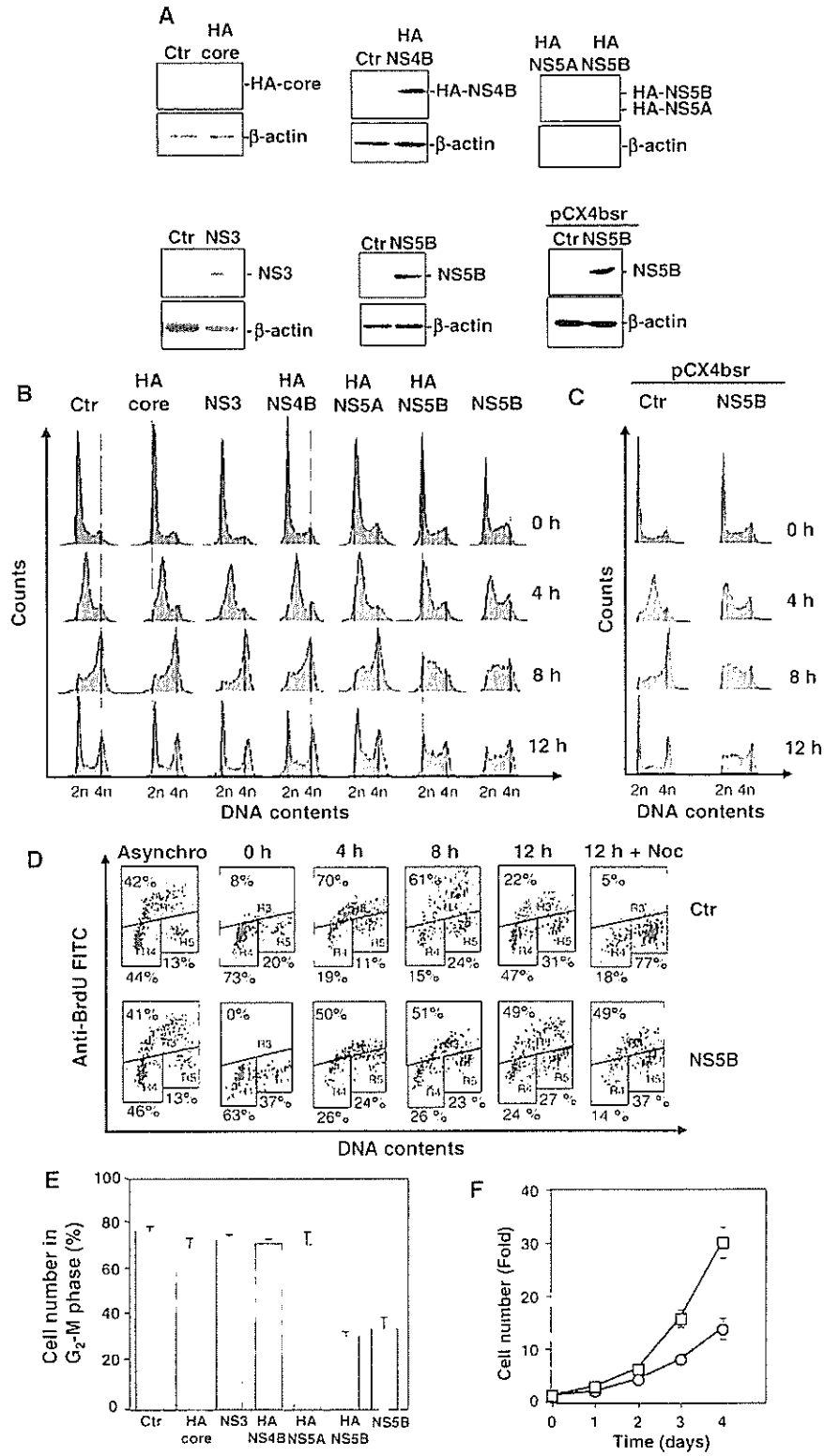

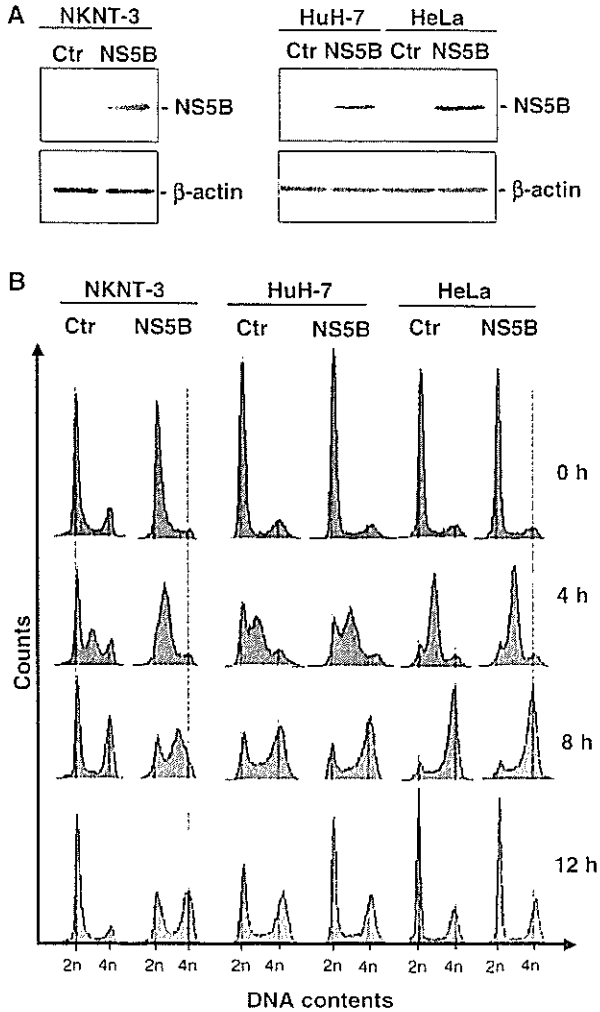

Fig. 2. NS5B delays S phase progression in another immortalized human hepatocytes. (A) Western blot analysis of NKNT-3, HuH-7, and HeLa cells infected with pCXbsr retrovirus encoding NS5B. The pCXbsr retrovirus was used as a control infection (Ctr). Anti-NS5B and anti-β-actin antibodies were used for the immunoblotting analysis. (B) Cell cycle analysis of NKNT-3, HuH-7, and HeLa cells expressing NS5B. NKNT-3, HuH-7, and HeLa cells that expressed NS5B (NS5B series) were synchronized, and cell cycle progression was analyzed as indicated in Fig. 1B. NKNT-3, HuH-7, and HeLa cells that were infected with the pCXbsr retrovirus were also analyzed as a control (Ctr series).

induced by NS5B. To evaluate this hypothesis, we examined whether or not PH/NS5B and NKNT-3 cells expressing NS5B (NK/NS5B) induce the expression of IFN-β. RT-PCR analysis clearly indicated that they did, and, at the same time, we found that HuH-7 and HeLa cells did not, despite their expression of NS5B (Fig. 3A). We next examined whether or not S phase progression is delayed in PH5CH8 and NKNT-3 cells treated with IFN-β prior to release from the G1/S boundary. As we expected, the S phase progression was stalled in PH5CH8 and NKNT-3 cells treated with IFN-β (Fig. 3B). We also observed that IFN-γ did not possess this activity of IFN-β (data not shown). These results suggest that the induction of IFN-β is implicated in the cell cycle delay in two immortalized human hepatocyte cell lines, PH5CH8 and NKNT-3.

To confirm the effect of IFN-β on cell cycle delay, we further examined whether or not treatment with anti-IFN-β neutralizing antibody can restore the cell cycle delay in PH/NS5B cells. The results showed that this treatment canceled the delay of S phase progression in PH/NS5B cells (Fig. 4A). BrdUrd incorporation analysis also showed that the proportion of cells reaching the G2-M phase was increased by the treatment with anti-IFN-β antibody in PH/NS5B cells (Fig 4B). These observations indicated that the expression of IFN-β mediated cell cycle delay during the S phase in PH/NS5B cells and suggested that the expression of NS5B induced IFN-β in PH5CH8 and NKNT-3 cells even without replication of the viral genome.

Activation of TLR3 signaling pathway by NS5B

Since IFN-β is known as a major cytokine induced by the activation of the TLR3 and TLR4 signaling pathways (Takeda et al., 2003), we next focused on which TLR pathway was activated for the production of IFN-β in PH/NS5B cells. To answer this question, TLR3- and TLR4-specific siRNAs were used to knock down TLR3 and TLR4 expression in PH/NS5B cells. TLR3 and TLR4 mRNAs were drastically decreased in PH/NS5B cells transfected with TLR3 and TLR4 siRNAs, respectively, but not in PH/NS5B cells transfected with GL2 siRNA (Elbashir et al., 2001) used as a control (Fig. 5A). This result indicates that the siRNAs used specifically contribute well to the degradation of TLR3 and TLR4 mRNAs. In this condition, IFN-β mRNA was significantly decreased in only PH/NS5B cells transfected with TLR3 siRNA (Fig. 5A), indicating that IFN-β expression in PH/NS5B cells is mediated through the TLR3 signaling pathway. The growth rate of PH/NS5B cells transfected with TLR3 siRNA was also accelerated, although TLR4 siRNA showed a rather lethal effect (Fig. 5B).

Fig. 1. HCV NS5B causes the delay of S phase progression. (A) Expression of HCV proteins in human cells introduced by retrovirus-mediated gene transfer. Western blot analysis of PH5CH8 cells infected with pCXbsr retroviruses encoding HCV proteins (HA-core, NS3, HA-NS4B, HA-NS5A, HA-NS5B, and NS5B) or pCX4bsr retrovirus encoding NS5B. pCXbsr or pCX4bsr retrovirus was used as a control infection (Ctr). Anti-HA (3F10, Roche), anti-NS3 (Novacastra), anti-NS5B, and anti-β-actin (Sigma) antibodies were used for the immunoblotting analysis. (B) Cell cycle analysis of PH5CH8 cells expressing HCV proteins. PH5CH8 cells that expressed HA-core, NS3, HA-NS4B, HA-NS5A, HA-NS5B, or NS5B were synchronized at G1/S boundary, and then cell cycle progression was monitored by flow cytometry after the release of the cells into the S phase at the indicated times. PH/Ctr cells that were infected with pCXbsr retrovirus were also analyzed as a control. (C) Cell cycle analysis of PH5CH8 cells infected with pCX4bsr retrovirus encoding NS5B. The cell cycle analysis was performed as described in panel B. (D) BrdUrd incorporation analysis of PH/Ctr and PH/NS5B cells. Cell cycle distribution of dot-plots of BrdUrd fluorescence versus DNA contents was analyzed in asynchronous or synchronized PH/Ctr and PH/NS5B cells. To measure the cells reaching the G2-M phase at 12 h after release, the cells were accumulated by Noc treatment. (E) Analysis of the cells reaching the G2-M phase. The percentage of cells at that phase was assessed by Noc treatment as indicated in panel D. The data are means ± SD of values from three independent experiments. (F) Growth curve of PH/Ctr and PH/NS5B cells. PH/Ctr (squares) or PH/NS5B (circles) were plated onto 6-well plates (3×10^4 cells per well), and the kinetics of cell proliferation during 4 days in culture were determined by trypan blue treatment. The data indicate average values ± SD from three independent experiments.

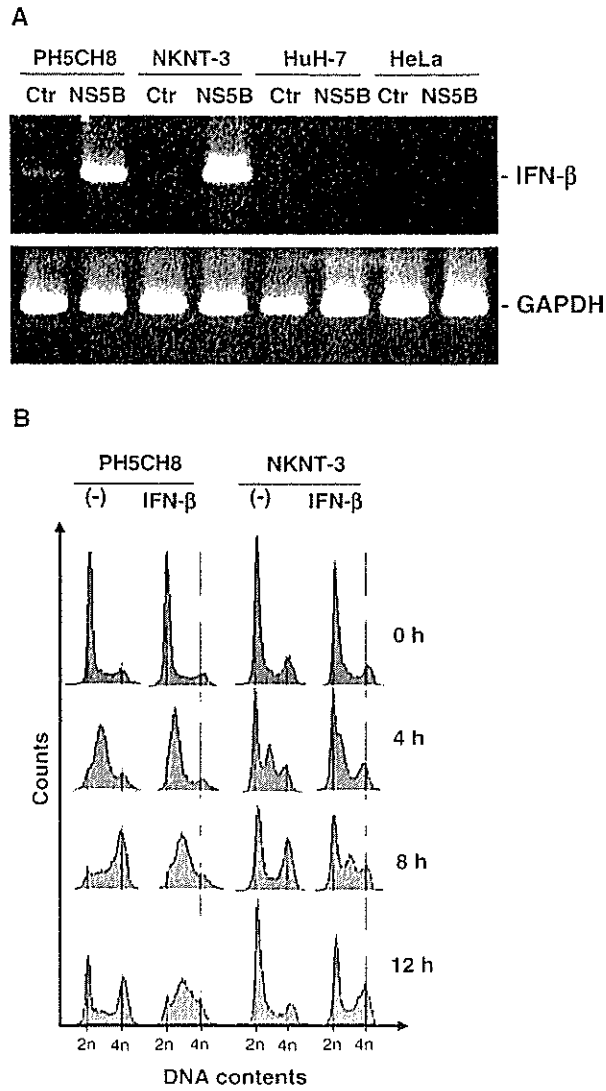

Fig. 3. IFN-β mediates the delay of S phase progression by NS5B. (A) RT-PCR analysis of IFN-β mRNA. The total RNAs were extracted from PH5CH8, NKNT-3, HuH-7, and HeLa cells (Ctr and NS5B series) and were subjected to RT-PCR analysis using primer sets for IFN-β (341 bp) and GAPDH (587 bp). (B) Cell cycle analysis of PH5CH8 and NKNT-3 cells treated with or without IFN-β. PH5CH8 and NKNT-3 cells were treated with or without IFN-β (500 IU/ml) at 12 h prior to release, and cell cycle progression was analyzed as indicated in Fig. 1B.

Furthermore, BrdUrd incorporation analysis using the Noc treatment revealed that 56% of PH/NS5B cells transfected with TLR3 siRNA reached the G2-M phase at 12 h after release, while only 33% of PH/NS5B cells transfected with GL2 siRNA reached that phase (Fig. 5C). The percentage of G2-M phase cells at 12 h after release was also 34% in PH/NS5B cells transfected with TLR4 siRNA, although the growth rate of these cells was lower than that of cells transfected with GL2 siRNA. These results indicated that the induction of IFN-β by NS5B expression was mediated through the activation of the TLR3 signaling pathway. This, in turn, demonstrated that TLR3 siRNA could override the delay of S phase progression in PH/NS5B cells.

To obtain further evidence that the induction of IFN-β by NS5B is mediated through TLR3, we prepared human embryonic kidney (HEK) 293 cells stably expressing TLR3 derived from PH5CH8 cells since it has been reported that ectopic expression of TLR3 can reconstruct the TLR3 signaling pathway in HEK293 cells (Alexopoulou et al., 2001). First, HEK293 cells were infected with retrovirus pCXbsr encoding NS5B or pCXbsr as a negative control (Ctr), yielding HEK293 cells (HEK/NS5B) stably expressing NS5B and control HEK293 cells (HEK/Ctr). Next, HEK/NS5B and HEK/Ctr cells were infected with

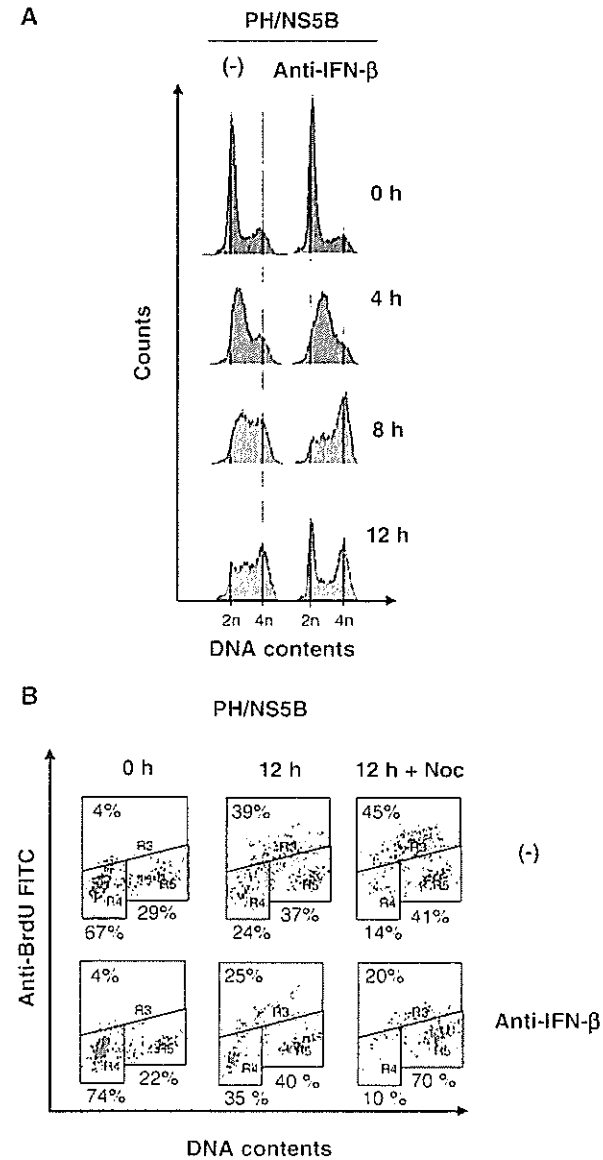

Fig. 4. Treatment with anti-IFN-β antibody canceled the delay of S phase progression. (A) Cell cycle analysis of PH/NS5B cells treated with or without anti-IFN-β antibody. PH/NS5B cells were treated with anti-IFN-β antibody (70 U/ml, Oxford Biotechnology) during cell cycle synchronization and after release from the G1/S boundary. (B) BrdUrd incorporation analysis of PH/NS5B cells treated with or without anti-IFN-β antibody. The antibody was used as indicated in panel A. Noc was used as indicated in Fig. 1D.